MARTIN MARIETTA ENERGY SYSTEMS LIBRARIES

3 4456 0054034 1

ORNL/TM-9677

ornl

OAK RIDGE
NATIONAL
LABORATORY

MARTIN MARIETTA

Analysis of Candidate Silicon Carbide Recuperator Materials Exposed to Industrial Furnace Environments

J. I. Federer
T. N. Tiegs
D. M. Kotchick
D. Petrak

OAK RIDGE NATIONAL LABORATORY
CENTRAL RESEARCH LIBRARY
CIRCULATION SECTION
4500N ROOM 175
LIBRARY LOAN COPY
DO NOT TRANSFER TO ANOTHER PERSON
If you wish someone else to see this report, send in name with report and the library will arrange a loan.

OPERATED BY
MARTIN MARIETTA ENERGY SYSTEMS, INC.
FOR THE UNITED STATES
DEPARTMENT OF ENERGY

Printed in the United States of America. Available from
National Technical Information Service
U.S. Department of Commerce
5285 Port Royal Road, Springfield, Virginia 22161
NTIS price codes—Printed Copy: A04; Microfiche: A01

This report was prepared as an account of work sponsored by an agency of the United States Government. Neither the United States Government nor any agency thereof, nor any of their employees, makes any warranty, express or implied, or assumes any legal liability or responsibility for the accuracy, completeness, or usefulness of any information, apparatus, product, or process disclosed, or represents that its use would not infringe privately owned rights. Reference herein to any specific commercial product, process, or service by trade name, trademark, manufacturer, or otherwise, does not necessarily constitute or imply its endorsement, recommendation, or favoring by the United States Government or any agency thereof. The views and opinions of authors expressed herein do not necessarily state or reflect those of the United States Government or any agency thereof.

ORNL/TM-9677
Dist. Category
UC-95

METALS AND CERAMICS DIVISION

ANALYSIS OF CANDIDATE SILICON CARBIDE RECUPERATOR MATERIALS EXPOSED TO INDUSTRIAL FURNACE ENVIRONMENTS

J. I. Federer, T. N. Tiegs,
D. M. Kotchick, and D. Petrak

Date Published — July 1985

Notice: This document contains information of a preliminary nature. It is subject to revision or correction and therefore does not represent a final report.

Prepared for the Assistant Secretary for Conservation and Renewable Energy, Office of Industrial Programs, Waste Energy Recovery Program

Prepared by the
OAK RIDGE NATIONAL LABORATORY
Oak Ridge, Tennessee 37831
operated by
MARTIN MARIETTA ENERGY SYSTEMS, INC.
for the
U.S. DEPARTMENT OF ENERGY
under Contract No. DE-AC05-84OR21400

MARTIN MARIETTA ENERGY SYSTEMS LIBRARIES
3 4456 0054034 1

CONTENTS

ABSTRACT 1
INTRODUCTION 1
EXPOSURE CONDITIONS 3
MATERIALS 10
RESULTS 13
APPEARANCE OF SPECIMENS 13
CHARACTERIZATION OF DEPOSITS 25
WEIGHT CHANGES 27
DIMENSIONAL CHANGES 27
MICROSTRUCTURAL VIEWS OF EXPOSED SURFACES 32
FLEXURE STRENGTH 51
DISCUSSION 52
SUMMARY 55
ACKNOWLEDGMENTS 56
REFERENCES 57

ANALYSIS OF CANDIDATE SILICON CARBIDE RECUPERATOR MATERIALS EXPOSED TO INDUSTRIAL FURNACE ENVIRONMENTS*

J. I. Federer, T. N. Tiegs,
D. M. Kotchick,† and D. Petrak‡

ABSTRACT

Several SiC ceramics were exposed to the combustion environments in six industrial furnaces to determine their corrosion resistance. The materials were sintered-α (Hexoloy SA), Sintride, recrystallized (NC-400), CVD SiC coated NC-400, siliconized (NC-430), reaction sintered (SC-X and KT), and Si_3N_4-bonded (C/75 and CN-178). Tubes of these materials were exposed in two aluminum remelt furnaces, a forge furnace, a steel reheat furnace, and two steel soaking pits at temperatures of 925 to 1250°C for periods of 530 to 5545 h. Significant corrosion occurred in specimens exposed to aluminum remelt furnaces and one of the steel soaking pits, whereas corrosion in the other furnaces was substantially less or negligible. The average C-ring fracture strengths of Hexoloy SA and NC-430, the only materials so tested, were substantially affected by the exposures. The lowest strength in Hexoloy SA occurred in specimens exposed in an aluminum remelt furnace, while the lowest strength in NC-430 occurred in specimens exposed in a steel soaking pit. These results show that SiC ceramics are susceptible to both corrosion and strength degradation when exposed to certain furnace environments.

INTRODUCTION

In recent years the Department of Energy has conducted research and development through industrial contractors to advance waste heat recovery technology. Two examples of this continuing effort are the ceramic

*Research sponsored by the Office of Industrial Programs, U.S. Department of Energy, under contract DE-AC05-84OR21400 with the Martin Marietta Energy Systems, Inc.

†AiResearch Manufacturing Company, 2525 West 190th Street, Torrance, CA 90509.

‡Babcock & Wilcox Company, P.O. Box 1260, Lynchburg, VA 24505.

recuperators developed by GTE Sylvania and Hague International for preheating combustion air. The GTE Sylvania ("Super Recuper") heat exchanger element is a multichannel crossflow cube fabricated of cordierite.[1,2,3] The recuperator consists of one or more cubes sealed in a housing with provisions for air and flue gas inlet and outlet flows. Numerous small passages for air and flue gases with thin partition walls result in a high effectiveness compared to radiant recuperators. Preheated air temperatures up to 800°C have been obtained. Although higher air temperatures could be obtained, the possibility of damage by softening of the cordierite is a serious concern. Because flue gas particulates tend to block the small passages, the GTE Sylvania recuperator is better suited for relatively clean combustion environments.[2]

The Hague International CerHx recuperator uses tubular oxynitride-bonded SiC heat exchanger elements with air to be preheated flowing through the tubes and flue gases flowing across the tubes in a crossflow mode.[4] Air preheat temperatures between 600 and 800°C are common. Large passages in the CerHx recuperator compared to those in the "Super Recuper" minimize the possibility of blockage by particle-laden flue gases.

Both the GTE Sylvania and Hague International recuperators have performed successfully on various industrial furnaces. Fuel savings averaged 44% for GTE Sylvania recuperators on 38 different furnaces[5] and ranged from 29 to 44% at nine host sites for Hague International recuperators.[6] Greater fuel savings, however, require even higher preheat temperatures. In 1982 the Department of Energy contracted with Garrett AiResearch Manufacturing Company* and Babcock & Wilcox Company to design, develop, build, and field test advanced high temperature burner-duct-recuperator (HTBDR) systems for preheating combustion air to 1090°C (2000°F).[7,8] This performance goal required that durable ceramic heat exchanger elements be fabricated and that energy losses by leakage through seals be minimized. Both contractors selected SiC ceramics as candidate materials for recuperator tubes on the basis of refractoriness and physical and mechanical properties; however, the corrosion resistance of the

---

*Funding for certain tasks was provided by the Gas Research Institute (GRI) in a cooperative program with DOE.

materials in various industrial furnace environments had not been determined.

The intended recuperator applications would involve recovery of waste heat from fouling, corrosive, flue gases in industrial furnaces such as steel reheat, steel soaking pit, and aluminum remelt furnaces. In these applications recuperator materials are exposed to flue gases containing numerous chemical species at temperatures up to 1300°C. Significant corrosion of recuperator tubes would adversely affect the economics of recuperation for a particular furnace because of tube replacement expense and furnace downtime. Both contractors used exposure tests, therefore, to assess the corrosion resistance of candidate materials. Garrett AiResearch installed specimens in five industrial furnaces for extended exposure tests, and Babcock & Wilcox installed specimens in a steel soaking pit, which represented the facility to be used for field testing. Subsequently, the specimens were analyzed at ORNL. Specimens were photographed, weighed, measured, and sectioned for ceramographic and electron microprobe examination of microstructures. Deposits were chemically analyzed and crystallographic compounds were identified by x-ray diffraction. Two materials, Hexoloy SA and NC-430, were subjected to flexure tests at 1100°C after exposure. The objective of these analyses and measurements was to correlate corrosion and changes in fracture strength with exposure conditions.

EXPOSURE CONDITIONS

The corrosion testing program involved installation of tubular specimens (except for a few bars) of SiC ceramics in six industrial furnaces for exposure to high temperature combustion environments. Although all furnaces burned natural gas, the composition of the flue gases depended on the type of furnace operation (as will be shown) and, possibly, on specific location within the flue. Table 1 shows the total period of specimen installation and the period of normal furnace use. The difference between these periods represents non-use periods, such as non-working shifts and weekends. During non-use periods the furnace temperatures were significantly lower than during normal use, while maximum

Table 1. Exposure conditions in industrial furnaces

Furnace	Exposure period		Maximum furnace temperature [°C (°F)]	Specimen location	Maximum estimated specimen temperature[c] [°C (°F)]
	Total[a] [h (days)]	Normal[b] [h (days)]			
Aluminum Remelt No. 1[d]	5545 (231)	5545 (231)	1040 (1900)	In flue ~2 ft from furnace	1040 (1900)
Aluminum Remelt No. 2[d]	1585 (66)	530 (22)	1150 (2100)	In flue ~3 ft from furnace	1150 (2100)
Steel Forge[d]	4440 (185)	4440 (185)	1175 (2150)	In center of furnace floor	1175 (2150)
Steel Reheat[d]	4370 (182)	1455 (61)	1300 (2375)	At flue exit ~4 ft from furnace	1100 (2010)
Steel Soaking Pit No. 1[d]	2280 (95)	2280 (95)	1345 (2450)	In flue ~24 ft from pit	925 (1700)
Steel Soaking Pit No. 2[e]	3460 (144)	3460 (144)	1250 (2300)	In flue ~1 ft from pit	1250 (2300)

[a]Total period of installation in the furnace.

[b]Period of normal furnace operation involving heating and cooling for loading and unloading.

[c]Occurring during normal furnace operation.

[d]Conducted by Garrett AiResearch.

[e]Conducted by Babcock & Wilcox.

estimated specimen temperatures (Table 1) occurred only during periods of normal use. Normal use, however, involved numerous heating and cooling cycles for loading and unloading the materials being processed. The maximum temperatures shown in Table 1, therefore, did not occur continuously during the normal use periods.

The exposures occurred during typical furnace operations involving feed materials, heating and cooling cycles, maximum temperatures, fluxes, and air-fuel mixtures. The aluminum remelt furnaces were charged with $NaCl$-KCl-Na_3AlF_6 flux along with metal to be melted. In addition, the molten aluminum in furnace No. 2 was sparged with chlorine gas during a portion of each normal cycle. The use of chlorine gas and chloride fluxes is normal industry practice for purifying scrap aluminum and for minimizing oxidation. The presence of chloride compounds in the flue gases, therefore, is not unusual. Steel billets in the soaking pits were covered with topping compounds, which is standard industry practice to minimize oxidation. Although flue gases in the furnaces were not analyzed, analysis of material that deposited on some specimens revealed significant quantities of metals (to be shown). Gaseous species in the fuel combustion products no doubt included N_2, O_2, CO_2, and H_2O.

Specimens were mostly exposed in crossflow configuration, that is, with the long axis perpendicular to the direction of flue gas flow. None of the specimens were exposed in the heat exchanger mode with air flowing through the inside. The combination of high temperature and medium length exposure time in steel soaking pit No. 2 represents one of the most severe thermal exposures among the group shown in Table 1.

The locations of each set of specimens are shown in Figs. 1–2 and 4–7. Specimens in aluminum remelt No. 1 were located in the flue near the furnace as shown in Fig. 1. The specimens were partially inserted into the refractory flue wall. Figure 2 shows that the specimens in aluminum remelt No. 2 were suspended from the roof of the flue near the furnace using a special hanger shown in the pretest condition in Figure 3. The hanger consisted of a SiC heating rod with a cement stop at one end and a metal holder clamped to the other end. Specimens in the steel forge furnace (Fig. 4) were located in the center of the floor, protected from

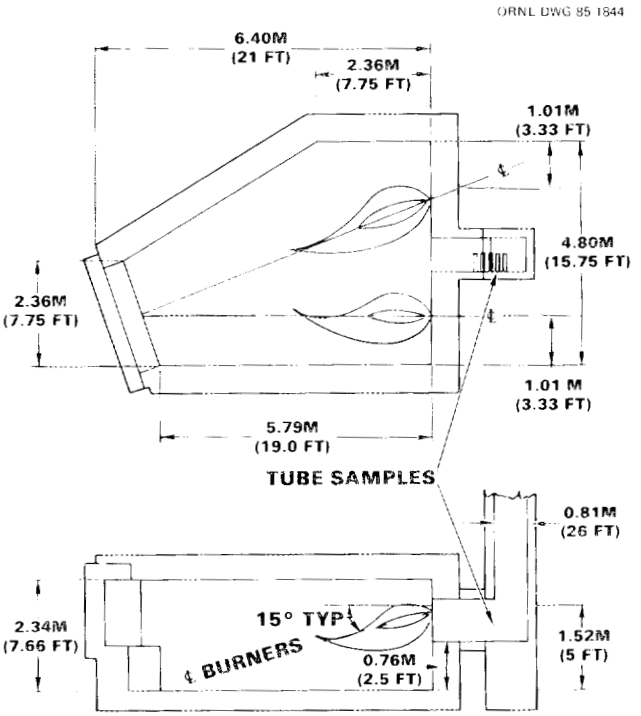

Fig. 1. Location of specimens in aluminum remelt furnace No. 1.

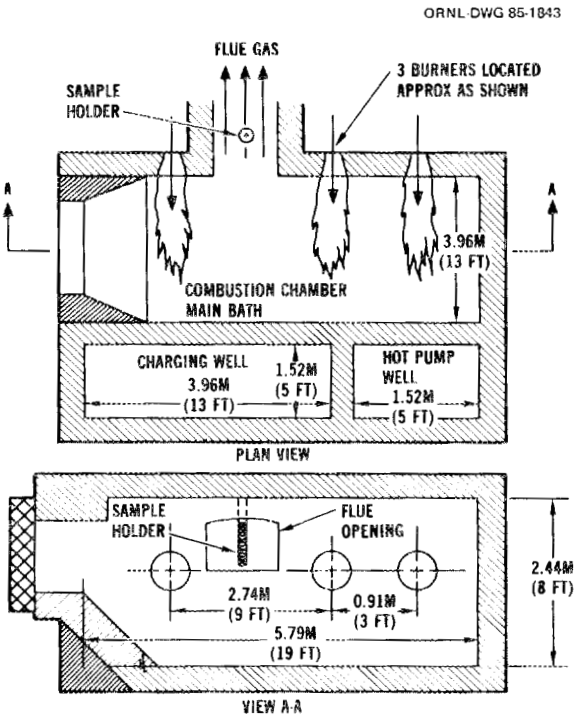

Fig. 2. Location of specimens in aluminum remelt furnace No. 2.

ORNL-PHOTO 1123-85

Fig. 3. Specimen holder for exposure testing in aluminum remelt furnace No. 2.

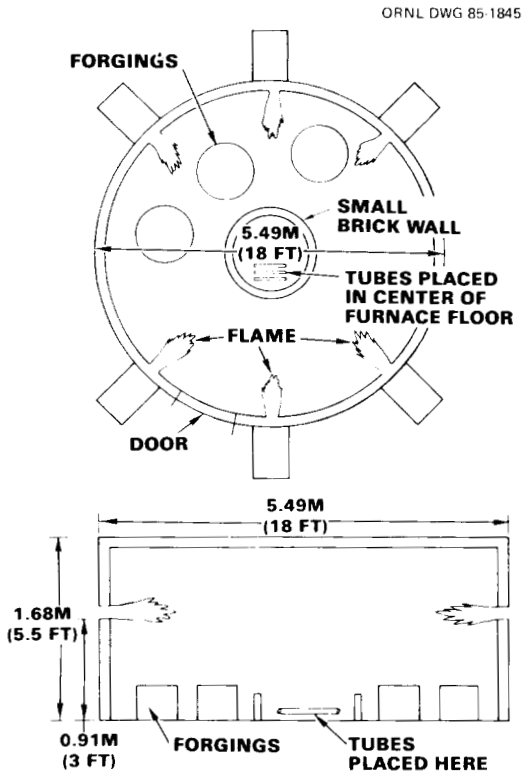

Fig. 4. Location of specimens in steel forge furnace.

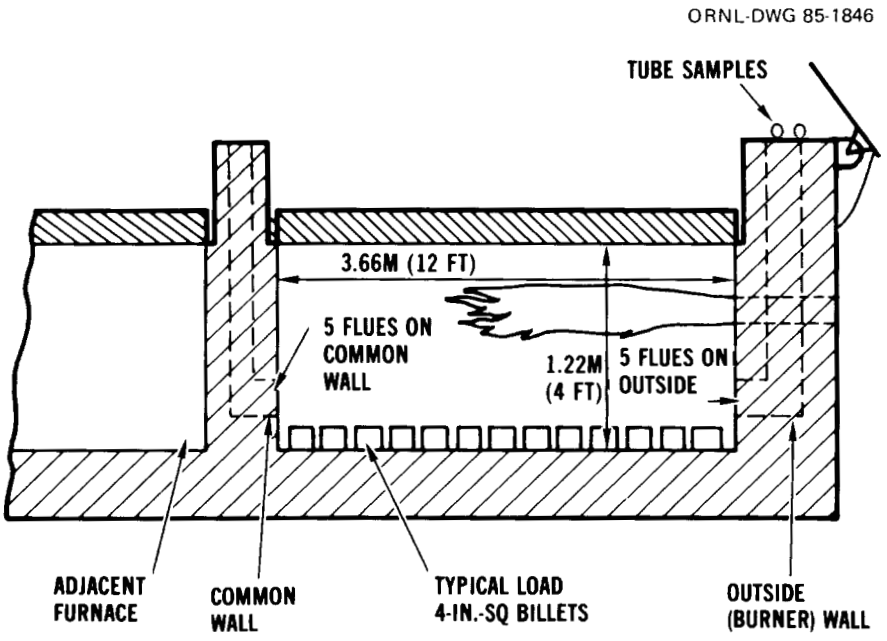

Fig. 5. Location of specimens in steel reheat furnace.

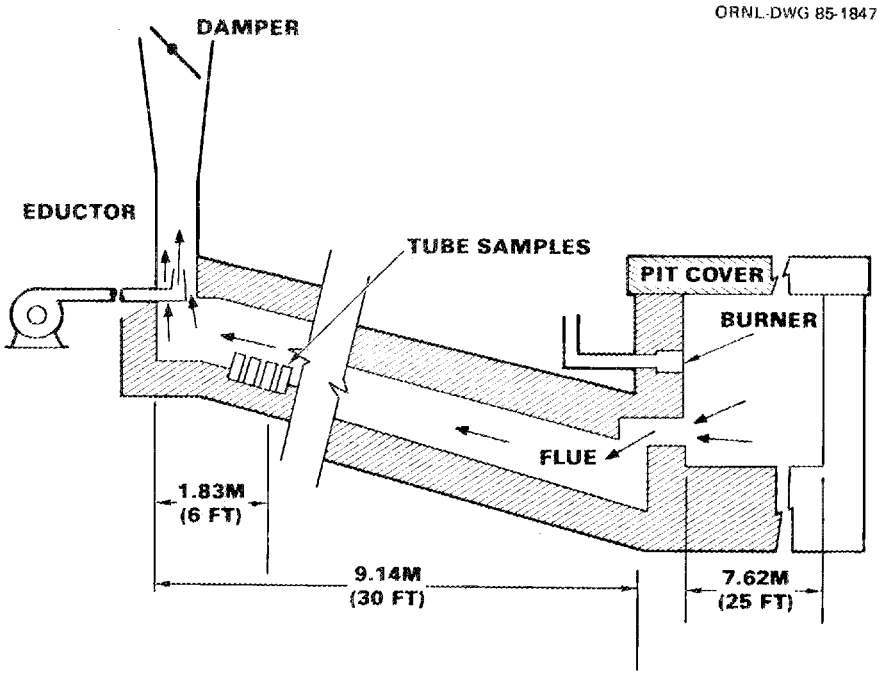

Fig. 6. Location of specimens in steel soaking pit No. 1.

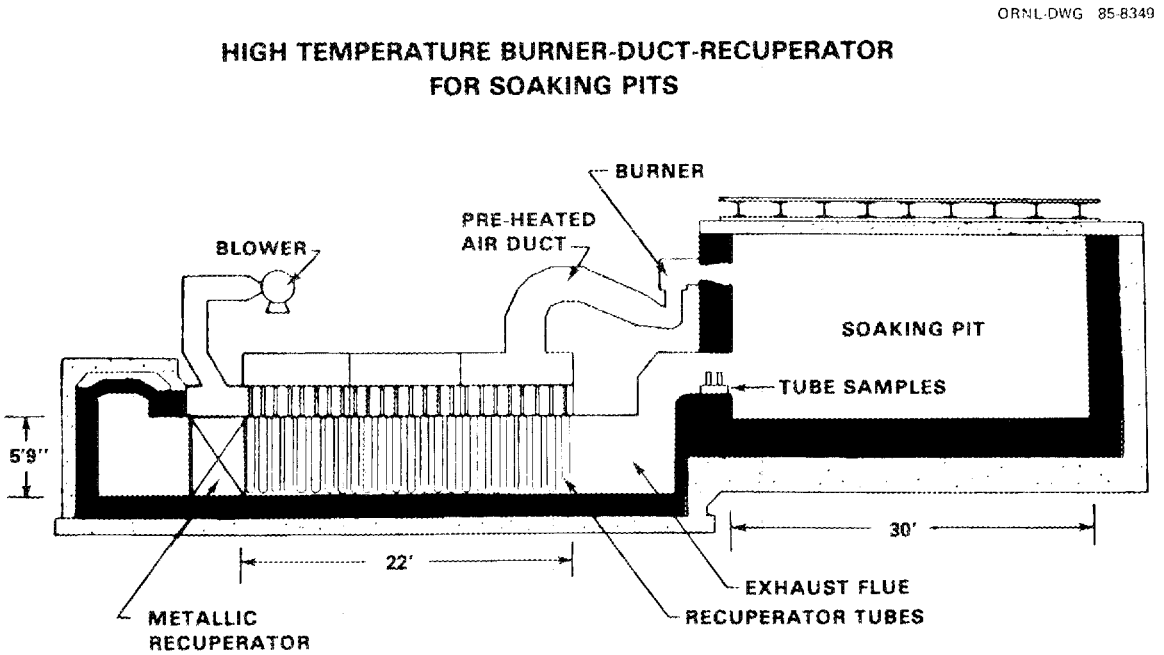

Fig. 7. Location of specimens in steel soaking pit No. 2.

direct contact with work pieces by a ring of refractory bricks. This location was used because flue openings were relatively small.

Specimens in the steel reheat furnace were located at the top of the flue (Fig. 5). Only the center portion of each specimen was exposed to flue gases in this arrangement. In steel soaking pit No. 1 the specimens were located in the flue approximately 7.3 m from the pit (Fig. 6). The specimens were inserted through the wall into the flue, and were retrieved by means of metal chains cemented into one end. Figure 7 shows the location of specimens in steel soaking pit No. 2. The specimens were positioned vertically in the flue about 0.3 m from the pit. This location, the only one available, provided a much more severe exposure than is anticipated for the actual recuperator. The recuperator, which will be located farther from the pit, will be exposed to lower temperatures and fewer entrained particulates because of one or more bends in the flue passage.

MATERIALS

Silicon carbide ceramics were selected as candidate materials for heat exchanger tubes and structural components in preference to oxide ceramics such as alumina and mullite.[7,8] Although the latter materials, especially alumina, are also strong and oxidation resistant, SiC is significantly less susceptible to thermal shock because of inherently higher thermal conductivity and lower coefficient of thermal expansion. The properties of SiC ceramics strongly depend on composition and density; therefore, several types were included in these exposure tests for comparison.

The exposed materials, shown in Table 2, represent most of the domestic commercially available SiC ceramics that might be considered for heat exchanger applications. Alumina and mullite were exposed in one furnace for comparison with the SiC ceramics. The specimens were mostly tubes measuring nominally 25 or 89 mm OD (1 or 3.5 in.) and 25 to 30 cm long (10 to 12 in.) except that the specimens in aluminum remelt No. 2 were only 5 cm long (2 in.). One Si_3N_4-bonded SiC (CN-178) was in the form of 15 mm × 15 mm × 25 cm bars. All materials were not included in each test. Some of the pretest specimens are shown in Fig. 8.

Table 2. Candidate materials exposed to industrial furnace environments

Type	Designation	Nominal composition, wt %	Manufacturer[a]
Sintered-α SiC	Hexoloy SA	>99 SiC	A
Sintered SiC	Sintride (SSIC)	>99 SiC	B
Recrystallized SiC	NC-400	>99 SiC	C
Recrystallized SiC coated with SiC	NC-400/CVD SiC	>99 SiC	C, D
Siliconized SiC	NC-430	90 SiC-10 Si	C
Siliconized SiC coated with Zircon[b]	NC-430/Zircon	90 SiC-10 Si	C
Reaction sintered SiC	SC-X	88 SiC-12 Si	E
Reaction sintered SiC	KT	84 SiC-16 Si	A
Si_3N_4-bonded SiC	C/75	75 SiC-23 Si_3N_4-2 oxide	F
Si_3N_4-bonded SiC	CN-178	75 SiC-23 Si_3N_4-2 oxide	C
Alumina	AD-998	99.8 Al_2O_3	E
Mullite	Mullite	72 Al_2O_3-28 SiO_2	E

[a]A — The Carborundum Company
B — General Electric Company
C — Norton Company
D — Garrett AiResearch
E — Coors Porcelain Company
F — NGK Locke, Inc.

[b]Zirconium silicate.

ORNL-PHOTO 0539-85

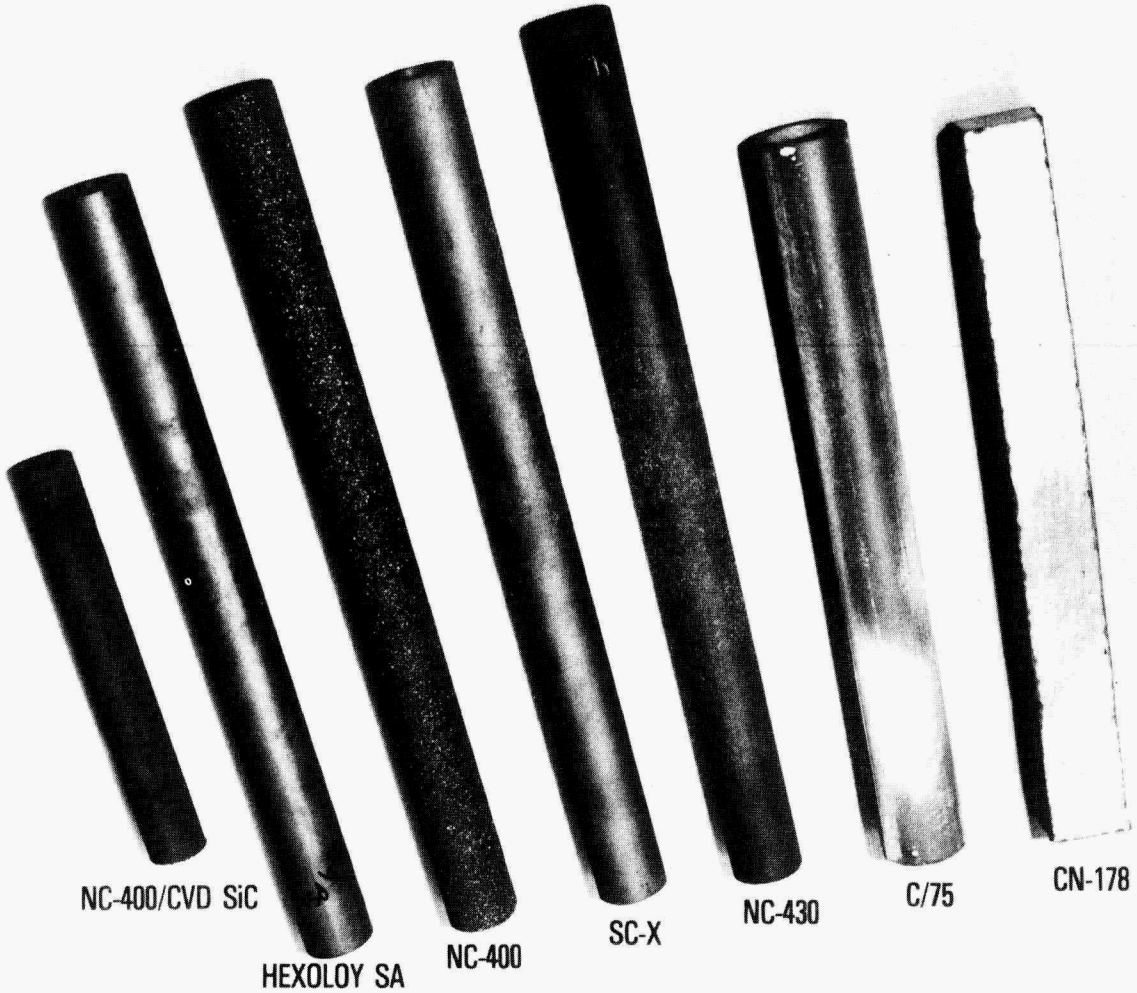

Fig. 8. Specimens for flue gas exposure in pretest condition.

Hexoloy SA (sintered-α SiC) and Sintride are highly pure and almost theoretically dense forms of SiC having the highest modulus of rupture (MOR) of any of the SiC ceramics. Recrystallized SiC (NC-400) is also highly pure, but is porous and much weaker than Hexoloy SA. This material was exposed both bare and with a dense SiC coating applied by chemical vapor deposition to the outer surface. Siliconized and reaction sintered SiC (NC-430, SC-X and KT) contain approximately 10 wt % Si. These materials, which consist of interpenetrating matrices of SiC and Si, have strengths that are intermediate to recrystallized SiC and Hexoloy SA. The Si_3N_4-bonded materials (C/75 and CN-178), which consist of large SiC grains bonded by a Si_3N_4 matrix, are considerably weaker than the other SiC ceramics. Alumina and mullite were also included in one furnace exposure (aluminum remelt furnace No. 1) for comparison with the SiC ceramics.

RESULTS

APPEARANCE OF SPECIMENS

The exposed specimens are shown in Figs. 9–20. Specimens exposed in the aluminum remelt furnaces were covered with deposits (Figs. 9–12), whereas specimens in the steel forge and reheat furnaces and soaking pit No. 1 were relatively clean as shown in Figs. 13–15. The deposit on the specimens in aluminum remelt furnace No. 1 (Figs. 9 and 10) was mostly porous and loosely adhering; however, a thin glassy layer was detected at the interface between deposit and SiC during microstructural examination. By contrast, the deposit on specimens in aluminum remelt furnace No. 2 (Figs. 11 and 12) was a glassy material, relatively rough in some areas and somewhat smoother at 180° locations. Specimens exposed in steel soaking pit No. 2 (Figs. 16–18) had a slag layer which was thickest on the downstream side. Slag on the upstream side was dull, but on the downstream side was glassy in appearance. High exhaust gas flowrates apparently forced molten slag, which deposited on the upstream side, to flow to the other side. Post exposure heating confirmed that the slag melted in the 1250 to 1300°C range. Extensive wall thinning can be observed in Fig. 18.

ORNL-PHOTO 0538-85

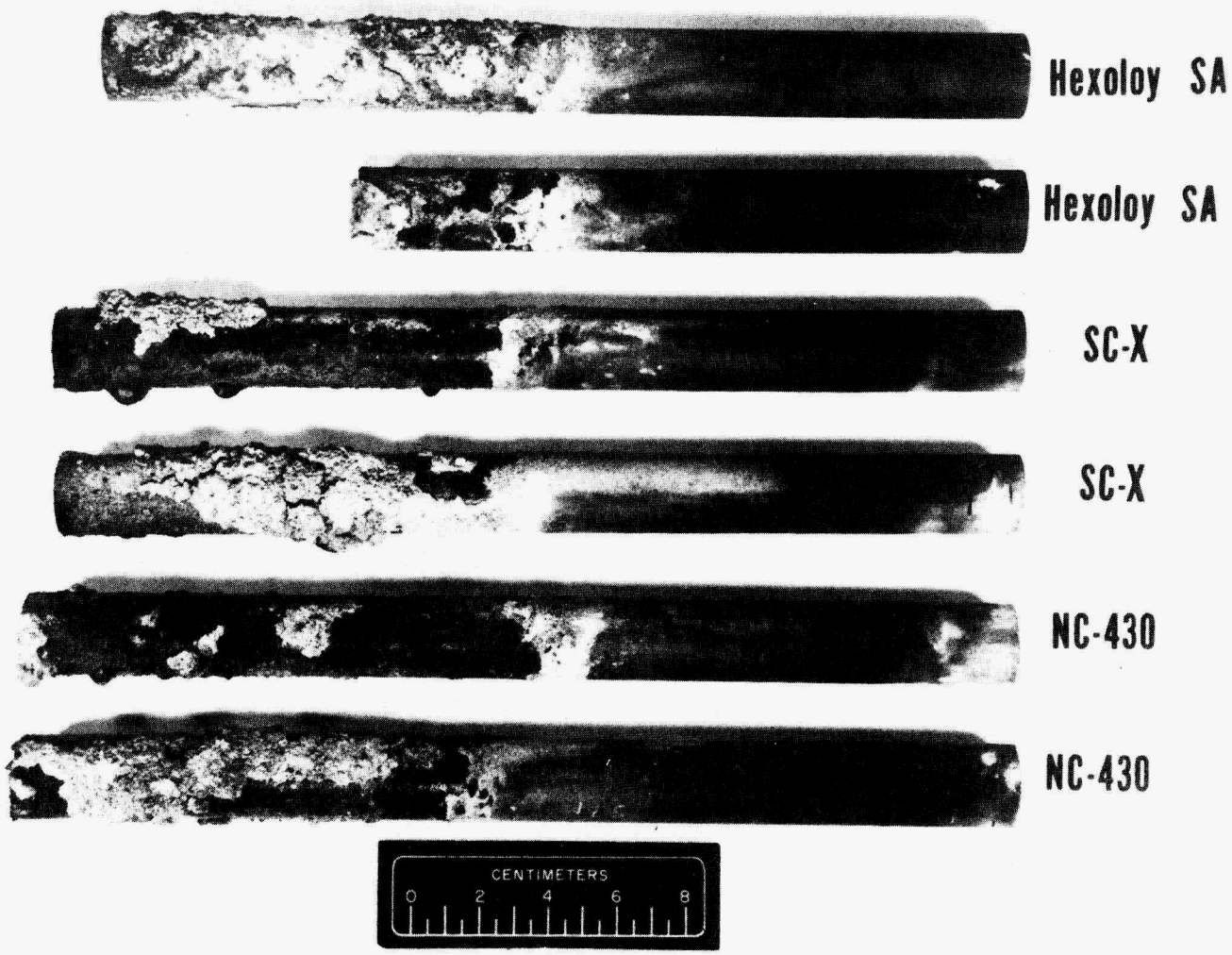

Fig. 9. Materials exposed in aluminum remelt furnace No. 1.

ORNL-PHOTO 0537-85

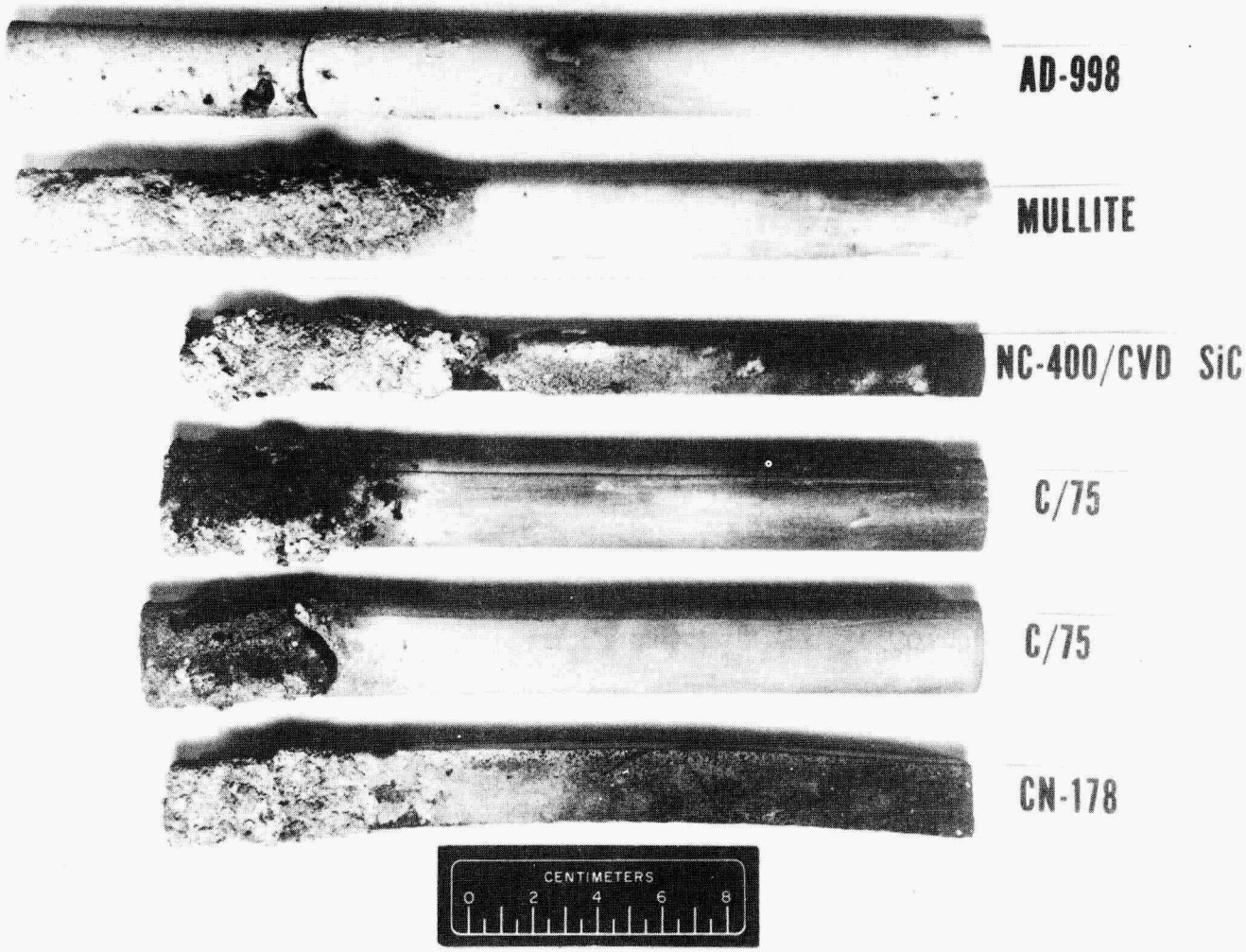

Fig. 10. Materials exposed in aluminum remelt furnace No. 1.

ORNL-PHOTO 0536-85

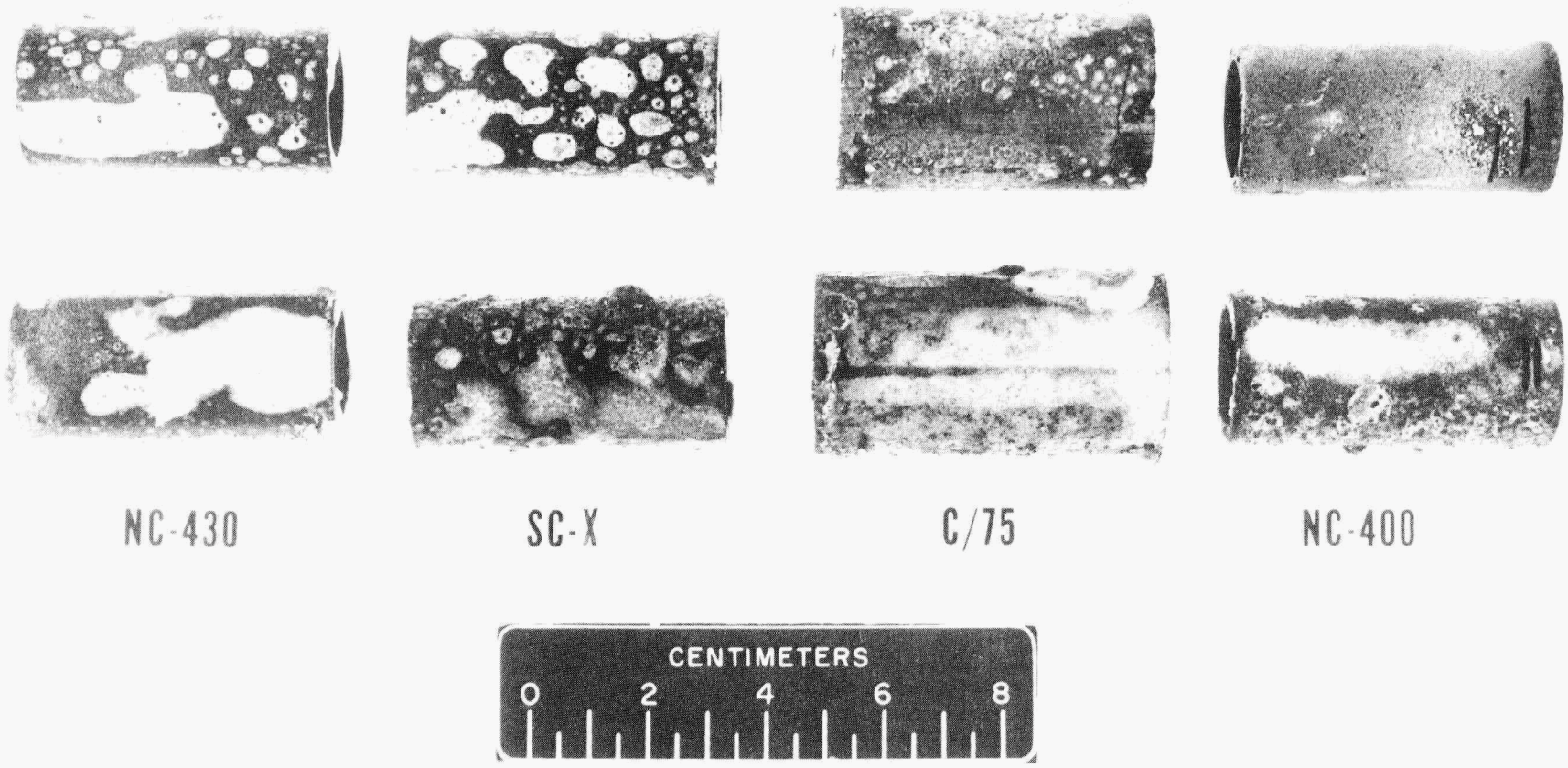

Fig. 11. SiC ceramics exposed in aluminum remelt furnace No. 2.

ORNL-PHOTO 0535-85

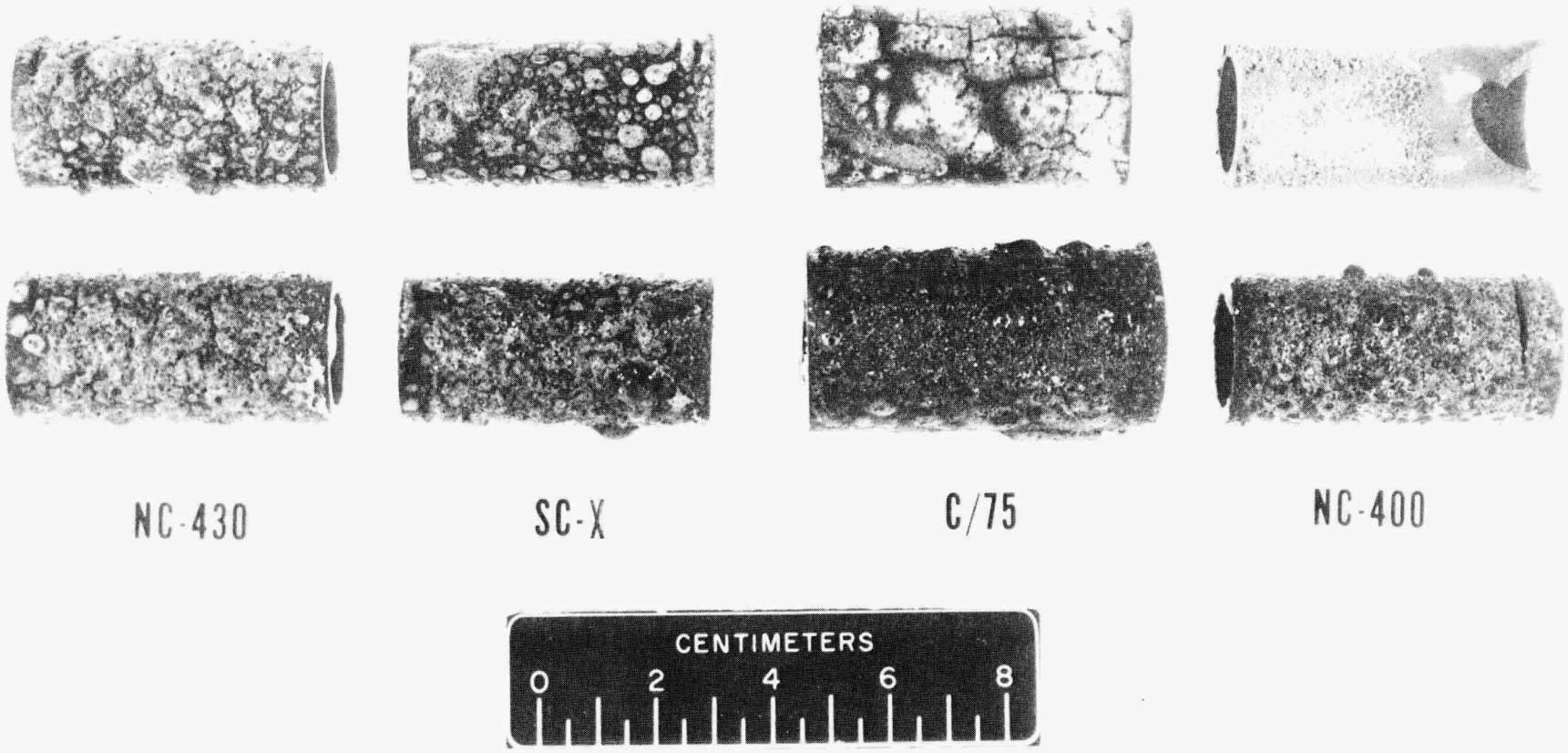

Fig. 12. SiC ceramics exposed in aluminum remelt furnace No. 2. Specimens are rotated 180° from the positions shown in Fig. 11.

ORNL-PHOTO 0534-85

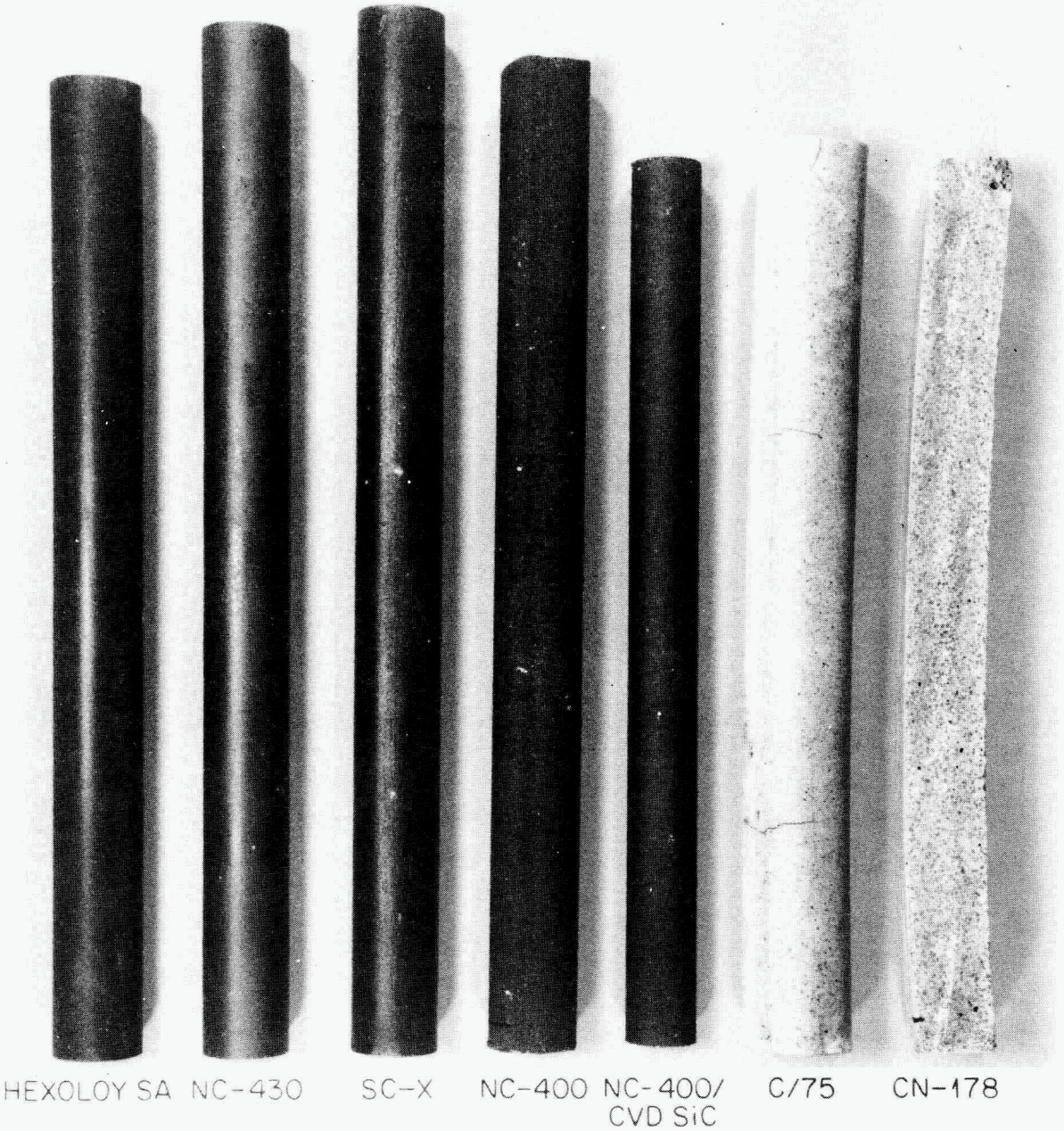

Fig. 13. SiC ceramics exposed in steel forge furnace. Also represents the appearance of specimens from the steel reheat furnace.

ORNL-PHOTO 0533-85

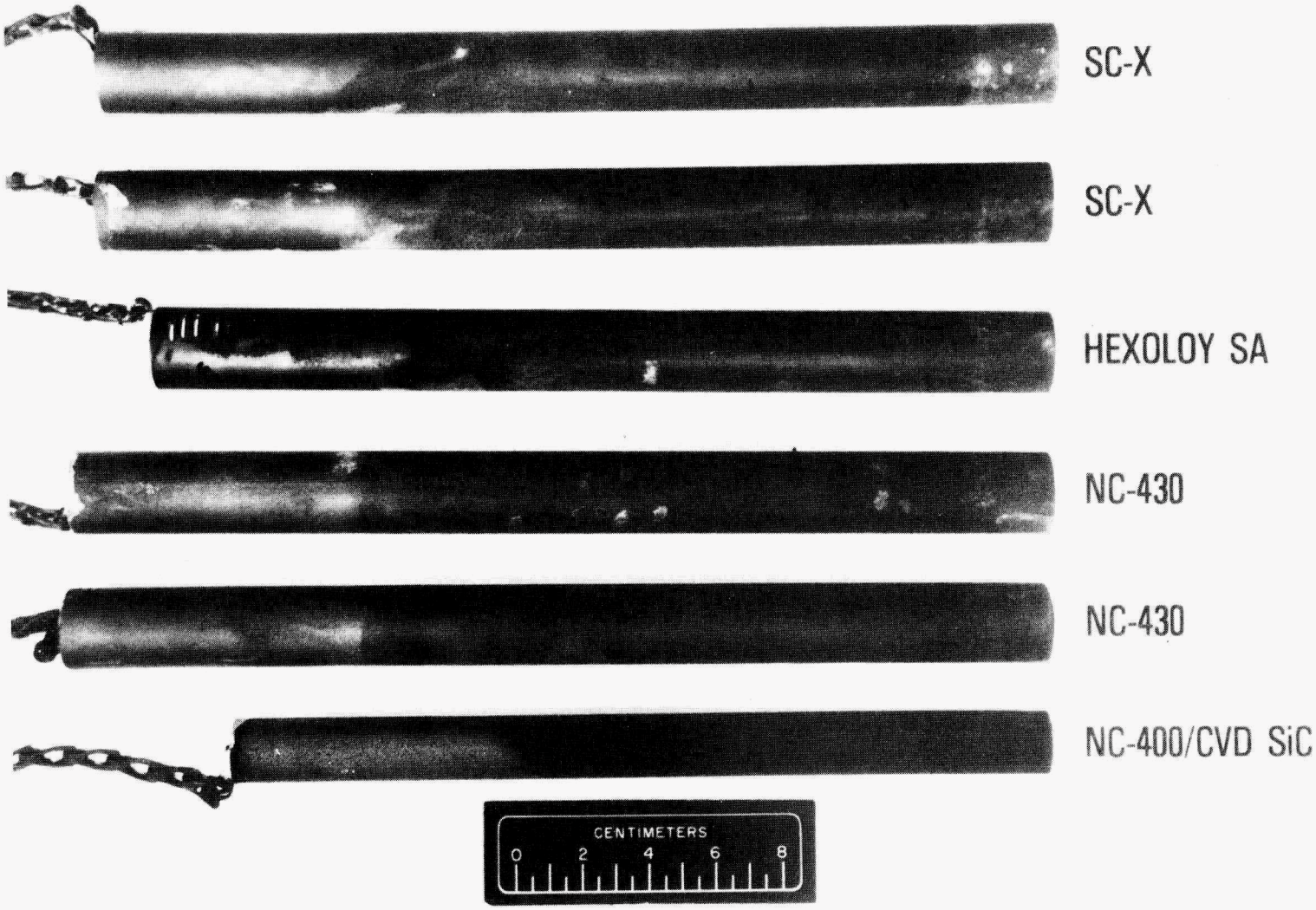

Fig. 14. SiC ceramics exposed in steel soaking pit No. 1.

ORNL-PHOTO 0532-85

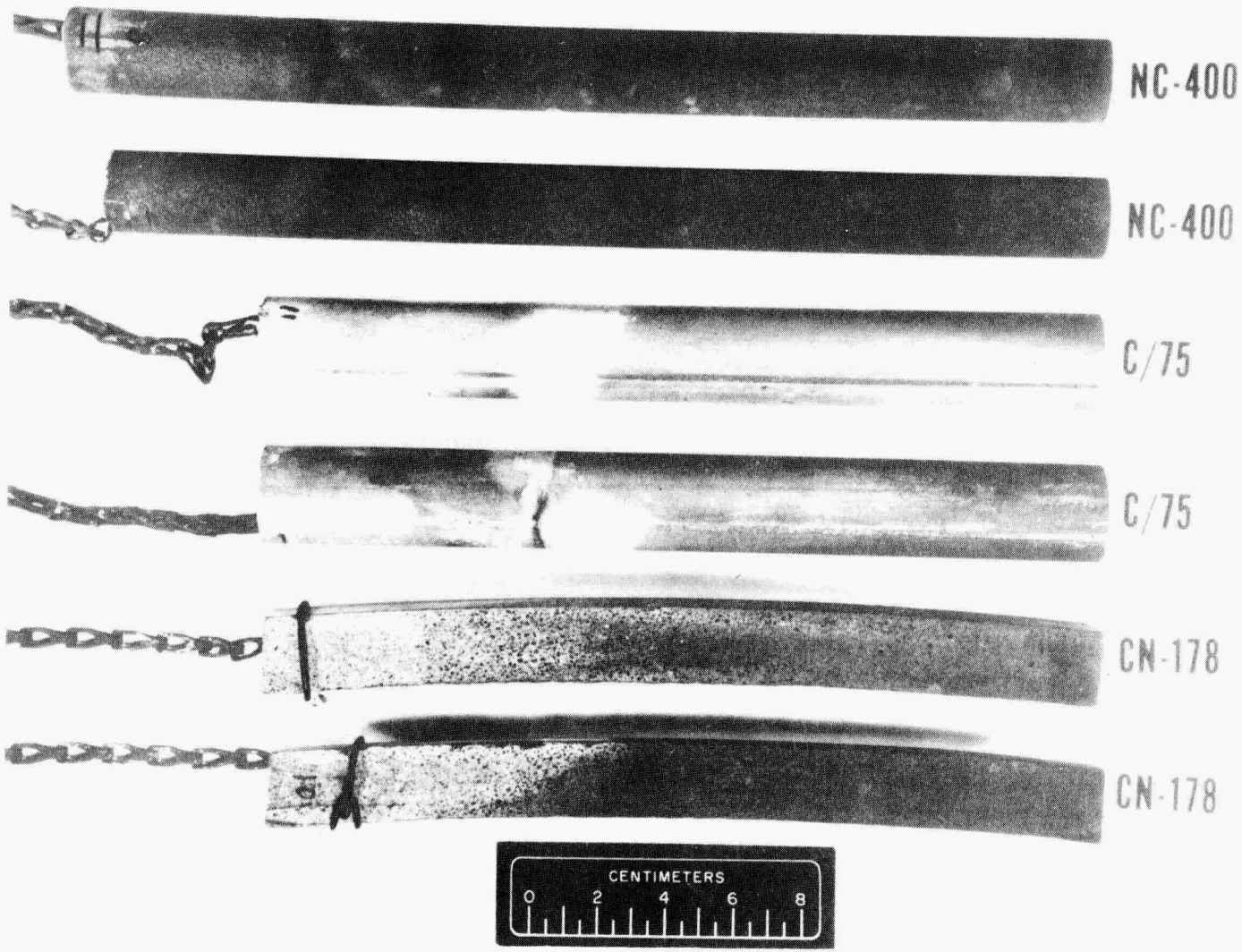

Fig. 15. SiC ceramics exposed in steel soaking pit No. 1.

ORNL-PHOTO 0530-85

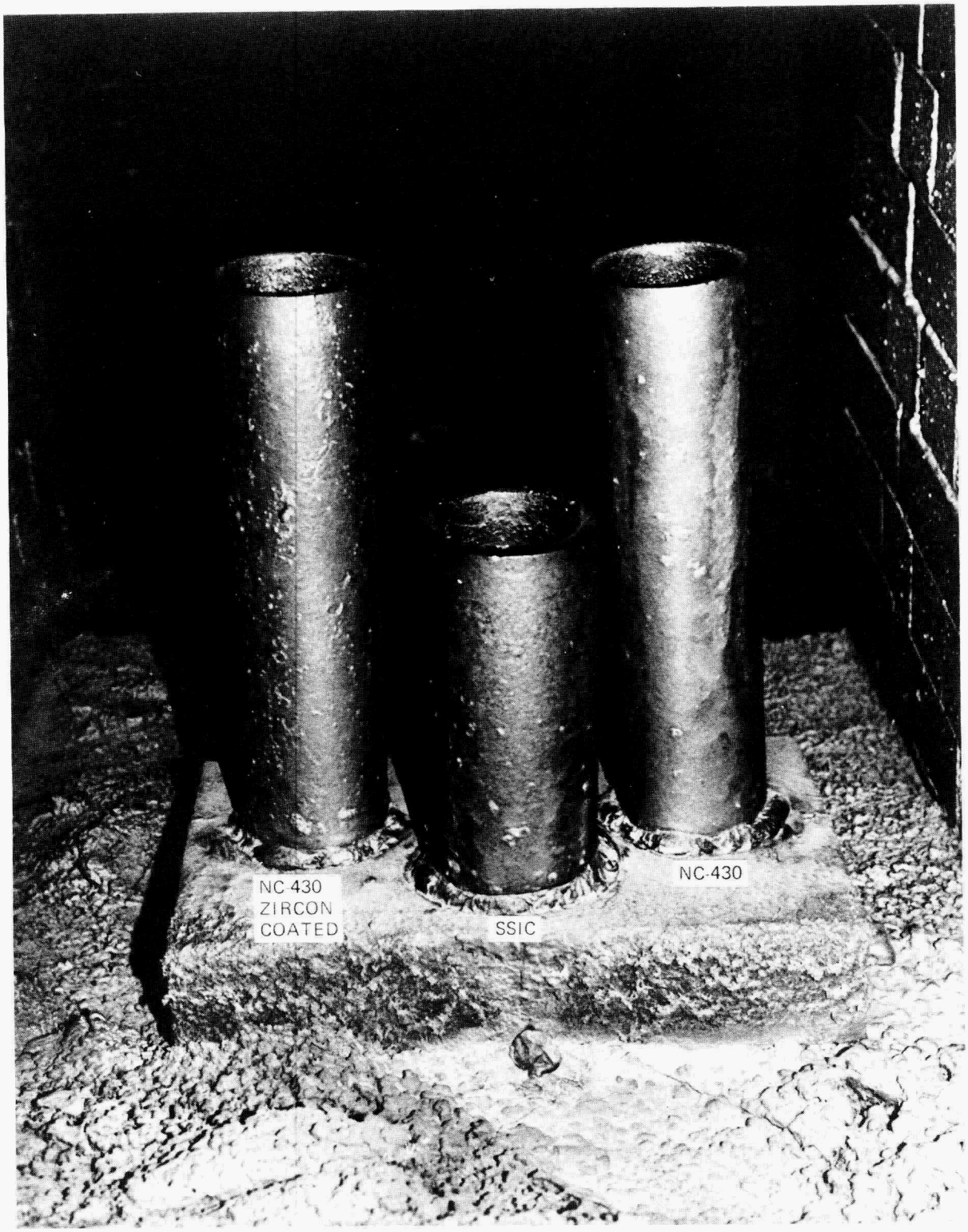

Fig. 16. SiC ceramics exposed in steel soaking pit No. 2.

ORNL-PHOTO 0531-85

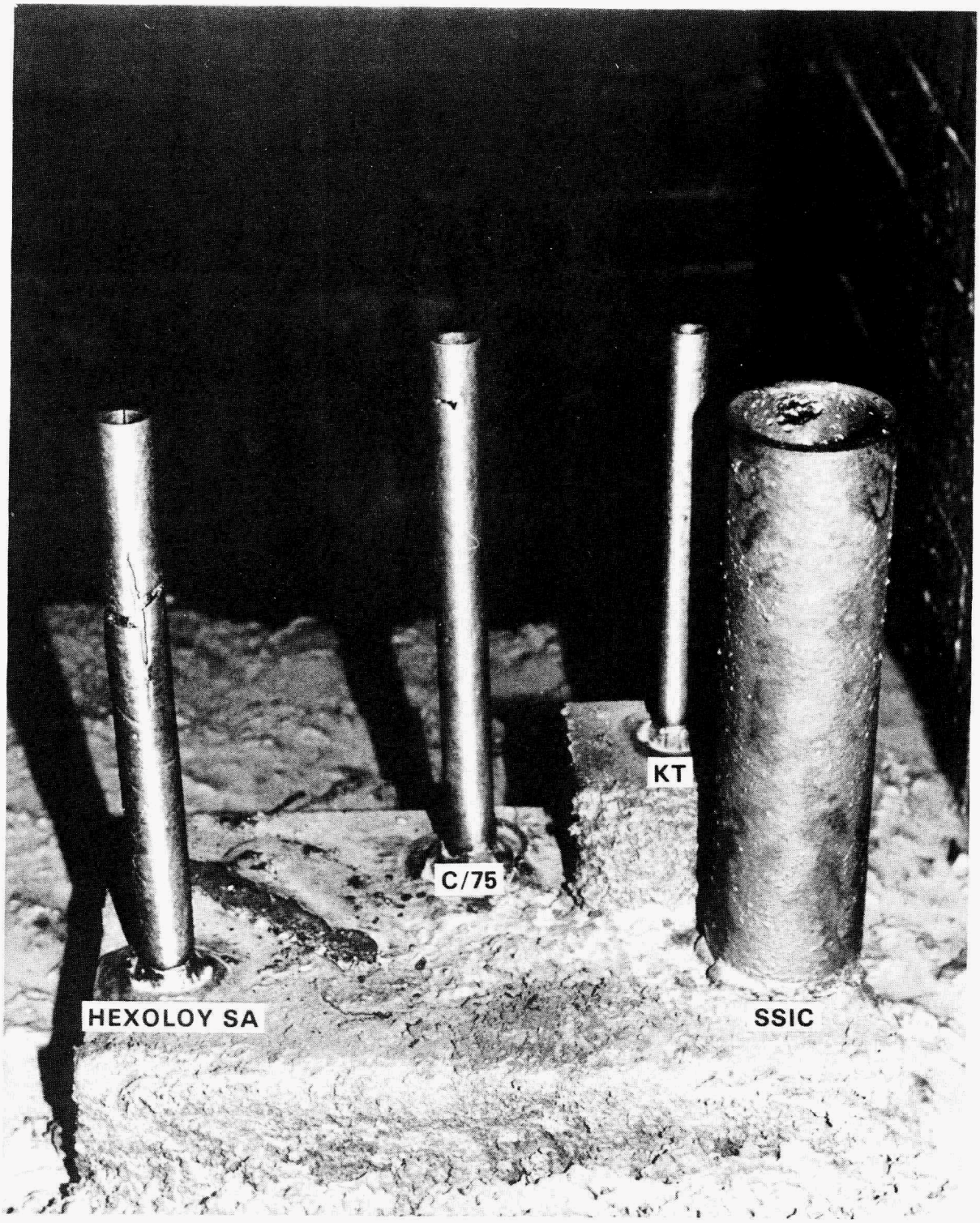

Fig. 17. SiC ceramics exposed in steel soaking pit No. 2.

ORNL-PHOTO 0525-85

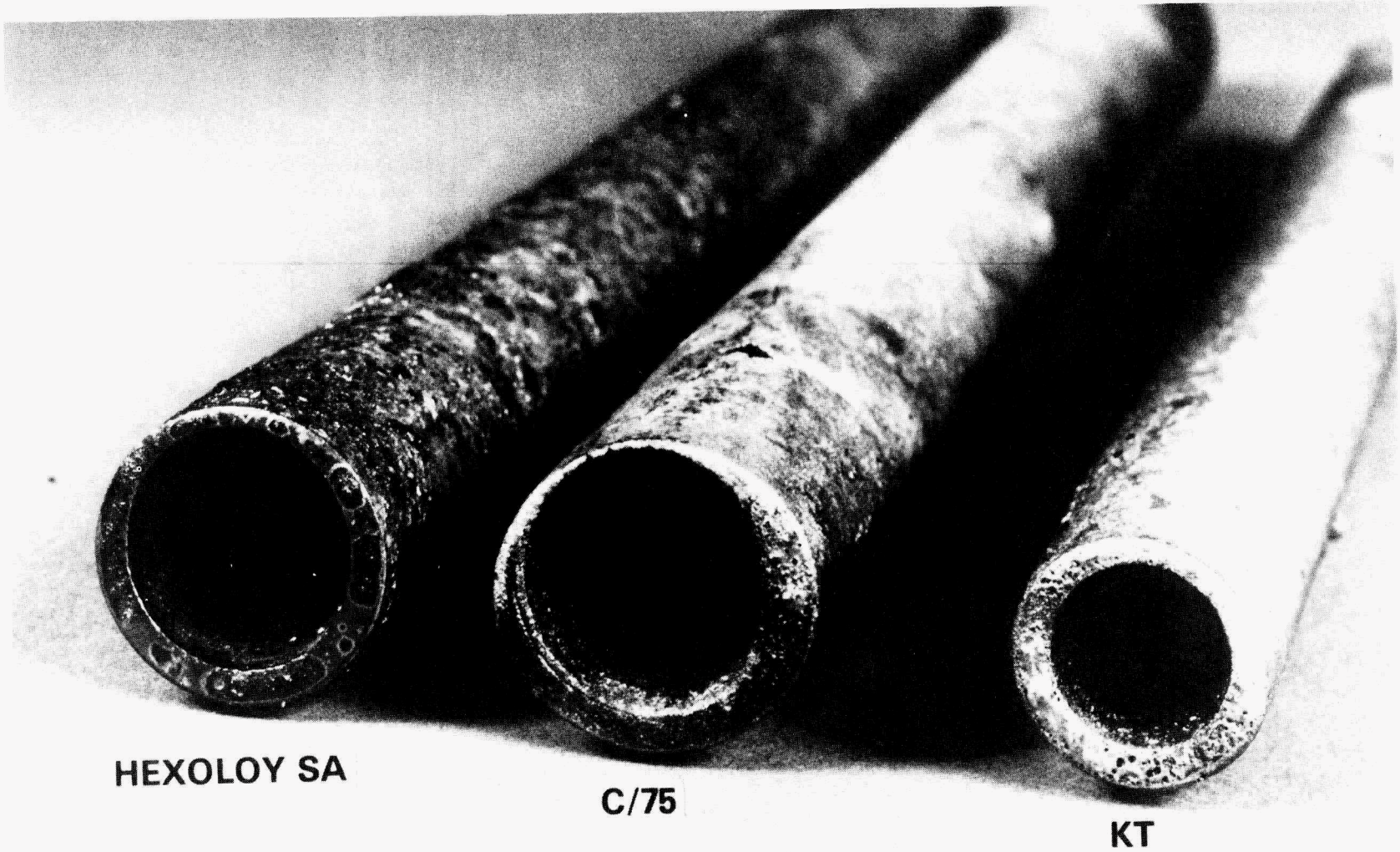

Fig. 18. SiC ceramics exposed in steel soaking pit No. 2.

ORNL-PHOTO 1124-85

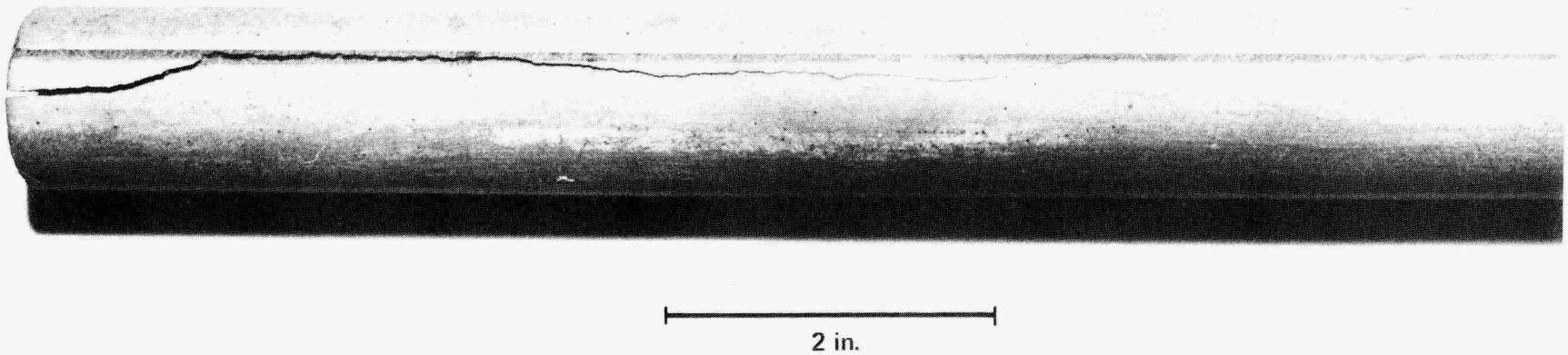

Fig. 19. Cracks in C/75 tube exposed in forge furnace.

ORNL-PHOTO 1125-85

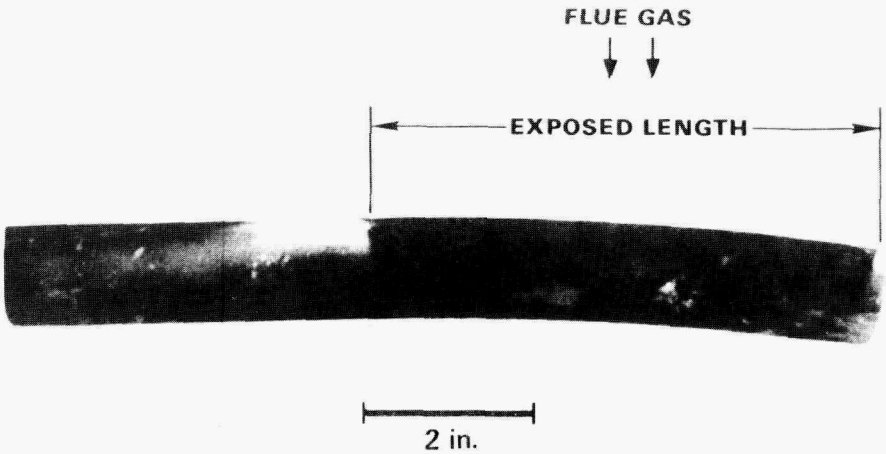

Fig. 20. Extensively deformed C/75 tube resulting from exposure in steel reheat furnace.

A few specimens broke during the exposures. One of each Hexoloy SA and C/75 specimens broke in aluminum remelt No. 1, as did the only AD-998 specimen. One NC-400 specimen broke in aluminum remelt No. 2. Cracking of Si_3N_4-bonded SiC specimens occurred in all exposures. The curvature of CN-178 bars, which is apparent in Figs. 10, 13, and 15, is the original shape of the bars, rather than the result of exposure. The C/75 material cracked extensively in most cases, as is evident in Fig. 19. Figure 20 shows extensive deformation in the C/75 material exposed to the steel reheat furnace environment.

CHARACTERIZATION OF DEPOSITS

The characteristics of deposits on specimens in three furnaces are shown in Table 3 (substantial deposits did not form in the other furnaces). The sources of elements in the deposits include the molten metal, flux, and furnace refractories. Potassium and sodium, in particular, were evidently derived from the NaCl-KCl flux that is used for purification and protection of the molten aluminum. The Cl content of deposits from both furnaces was lower than that of K and Na, indicating that NaCl and KCl reacted with other species to produce chloride compounds having high vapor pressures.

Table 3. Characteristics of deposits on specimens exposed to industrial furnace environments

Content,[a] ppm	Aluminum remelt No. 1	Aluminum remelt No. 2	Steel soaking pit No. 2
	Composition		
Major[b]	Al, Si	Al, K, Na, Si	Cr, Fe, Si
1000–3000	Fe, K, Na, Zn	Ba, Ca, Cu, Fe, Zn	Cu, K, Mn
500–1000	Ca, Ti	Cl, Mg	Ca, Na, Ni
100–500	B, Ba, Bi, Cr, Cu, Mg, Mn, Ni, P, Pb, S, Sn	Mn, S, Sr	P, S, Ti, Zn
<100	Ce, Cl, Co, Mo, Sc, V, Zr	B, Co, Cr, F, La, Mo, Ni, P, Rb, Ti, V, Zr	As, B, Cl, Co, Ga, Ge, Mg, Mo, Rb, V, Zr
	Crystalline Compounds		
	Al_2O_3	(Ca, Mg, Fe, Al) silicate	
	$Na_2O \cdot Al_2O_3 \cdot 2SiO_2$		
	Melting Range, °C		
	1200–1300	1150–1300	1250–1300

[a]Determined by semiquantitative spectrographic analysis.

[b]5 to 20%.

[c]Not determined.

X-ray diffraction of the deposit on specimens in aluminum remelt No. 1 revealed the presence of alumina and nepheline (or carnegieite) as shown in Table 3. The presence of alumina (Al_2O_3) is consistent with the high Al content revealed by chemical analysis. The melting temperature of carnegieite ($Na_2O \cdot Al_2O_3 \cdot 2SiO_2$) of stoichiometric composition is approximately 1525°C. This compound, and its lower temperature modification nepheline, exist over a wide range of compositions in the Na_2O-Al_2O_3-SiO_2 system with melting temperatures ranging below 800°C. The presence of several other compounds also was indicated by x-ray diffraction: potash feldspar ($K_2O \cdot Al_2O_3 \cdot 6\ SiO_2$), magnetite ($Fe_3O_4$), zinc

aluminate ($ZnO \cdot Al_2O_3$), and calcium hexaluminate ($CaO \cdot 6\ Al_2O_3$). The x-ray evidence, however, was not strong enough to confirm the presence of these compounds. Only one crystalline compound, (Ca, Mg, Fe, Al) silicate, was revealed by X-ray diffraction of the deposit on specimens in aluminum remelt No. 2 in spite of the fact that Ca, Fe, and Mg were not among the most abundant elements. This deposit consisted mainly of a silicate glass containing K and Na in solution, as will be shown. Many elements in the deposit on specimens in steel soaking pit No. 2 were derived from the steel billets being heated (e.g., Cr, Fe, Si, Mn and Ni) and from topping compounds.

The melting range for the deposits was determined by stepwise heating. Table 3 shows that melting occurred in the 1150 to 1300°C range. Specimens in aluminum remelt No. 2 and steel soaking pit No. 2 had evidently been exposed to such temperatures because the deposits had obviously been molten.

WEIGHT CHANGES

Weight changes occurring in specimens in the forge and steel reheat furnaces are presented in Table 4. Specimens in these furnaces apparently were exposed to relatively clean atmospheres compared to those in the aluminum remelt furnaces because no deposits were evident on the surfaces. The weight changes in these specimens, therefore, were probably caused by oxidation. Table 4 shows that the Si_3N_4-bonded materials had significantly higher weight changes (gains) than the other specimens. Even the porous NC-400 and the materials containing silicon as a primary phase (NC-430 and SC-X) had smaller weight gains than the Si_3N_4-bonded materials. The weight gains exhibited by C/75 and CN-178 are tentatively attributed to oxidation of the Si_3N_4 bonding phase in these ceramics. This oxidation might have caused the previously mentioned extensive cracking of some specimens of these materials.

DIMENSIONAL CHANGES

The outer diameters of exposed specimens were measured to determine changes indicative of corrosion. Measurements were made with a micrometer

Table 4. Weight changes of SiC ceramics exposed to industrial furnace environments

Material		Weight change, %	
Type	Designation	Steel forge furnace (1175°C, 2150 h)	Steel reheat furnace (1100°C, 2010 h)
Sintered-α	Hexoloy SA	0	0.2
Recrystallized	NC-400	-0.1	0.2[a] 0.1[a]
Recrystallized/CVD coated	NC-400/CVD SiC		0.6
Siliconized	NC-430	0	0.4[a] 0.5[a]
Reaction sintered	SC-X	0	0.5
Si_3N_4-bonded	C/75	17.5	4.2[a] 1.9[a]
	CN-178	3.8	1.4

[a]Two specimens in exposure test.

on apparently clean specimens, i.e., those from the forge, steel reheat, and steel soaking pit furnaces. Specimens from the aluminum remelt furnaces, as previously mentioned, had deposits on the surfaces, which required that their diameters be measured with a microscope on samples prepared for ceramographic examination. In either case three or four measurements were made at approximately equal intervals around the circumference. Unfortunately, the pretest specimens had been only nominally measured before exposure. The measurements on exposed specimens, therefore, were not necessarily in the same locations as pretest measurements. In addition, some types of materials consisted of tubes from different lots that differed slightly in diameters.

The ends of specimens were protected from the furnace environments by the holding arrangements in aluminum remelt No. 1, steel reheat, and steel soaking pit No. 1. The ends of these specimens were measured to obtain representative pretest diameters for comparison with exposed specimens. This method is subject to error if tube diameters are not uniform along the length; however, the absence of better information required that this

method be used. The protected diameters of these specimens were averaged to obtain representative pretest diameters of specimens that could not be measured directly.

The measurements of specimen diameters are presented in Table 5, and the corrosion rates calculated from these measurements are summarized in Table 6. These results show that significantly more corrosion occurred in specimens exposed to aluminum remelt furnace and steel soaking pit No. 2 environments than in the other furnaces. The corrosion rate was significantly higher in aluminum remelt No. 2 than in aluminum remelt No. 1.

The higher rate in aluminum remelt No. 2 might be associated with a much shorter exposure time (since corrosion rates sometimes decrease with increasing time) or with a higher temperature. Specimens in the forge and steel reheat furnaces and in steel soaking pit No. 1 had relatively small corrosion rates, which probably represent measuring uncertainty. A possible exception is NC-430, which exhibited surface recession in each exposure test.

The specimens in the aluminum remelt furnaces were covered with adherent glass deposits (also loosely adherent deposits in No. 1). The surface deposits might have participated in corrosion in these specimens. The data also indicate that the siliconized SiC ceramics (NC-430 and SC-X) corroded more than pure SiC (Hexoloy SA and NC-400) in the aluminum remelt furnaces.

Specimens in steel soaking pit No. 2 were covered with slag, which was thickest on the downstream side. The largest dimensional changes (reported in Table 6) occurred on the upstream side. The specimens in this test exhibited much larger dimensional changes than those in the other tests, especially steel soaking pit No. 1. In the latter case the specimens were exposed to substantially lower temperatures and had no significant surface deposits, apparently because of a more protected location in the flue.

No dimensional changes were determined for several specimen types: NC-400/CVD SiC because the coated surfaces were too rough to obtain accurate pretest diameters; C/75 (except one sample from steel soaking pit No. 2) because this material either corroded extensively or cracked and swelled; CN-178 because of difficulty in determining pretest dimensions

Table 5. Summary of diameter changes of SiC ceramics exposed to industrial furnace environments

Specimens	Average specimen diameters,[a] mm							
	Aluminum remelt No. 1		Aluminum remelt No. 2	Steel forge	Steel reheat	Steel soaking pit No. 1		Steel soaking pit No. 2
Hexoloy SA								
Pretest	25.78[b]	25.40[b]	--	25.55[c]	25.27	25.60		24.77
Posttest	25.50	24.97	--	25.60	25.22	25.58		23.93
Change	-0.28	-0.43	--	+0.05	-0.05	-0.02		-0.84
NC-400								
Pretest	25.04		25.35[c]	25.35[c]	25.55	25.07[b]	25.53[b]	--
Posttest	24.87		24.89	25.50	25.55	25.02	25.60	--
Change	-0.17		-0.46	+0.15	0	-0.05	+0.07	--
NC-430								
Pretest	25.55[b]	24.99[b]	25.02[c]	25.02[c]	25.63	25.04[b]	25.60[b]	88.93
Posttest	24.99	24.49	24.79	24.89	25.40	25.02	25.45	87.63
Change	-0.56	-0.50	-0.23	-0.13	-0.23	-0.02	-0.15	-1.30
SC-X								
Pretest	24.84[b]	24.99[b]	24.92[c]	24.92[c]	24.84	24.94[b]	24.89[b]	--
Posttest	24.18	24.26	24.64	24.99	24.92	24.92	24.97	--
Change	-0.66	-0.73	-0.28	+0.07	+0.08	-0.02	+0.08	--
C/75								
Pretest	--	--	--	--	--	--	--	26.54
Posttest	--	--	--	--	--	--	--	24.43
Change	--	--	--	--	--	--	--	-2.11

[a]Values are averages of four measurements.

[b]Two specimens in same test.

[c]Average of specimens in other furnaces because these could not be measured directly.

Table 6. Corrosion rates of SiC ceramics exposed to industrial furnace environments

Furnace	Maximum temperature (°C)	Time (h)	Corrosion rate,[a] pm/s						
			Hexoloy SA	Sintride	NC-400	NC-430	SC-X	KT	C/75
Aluminum Remelt No. 1	1040	5545	-8.9 (-0.3)[d]	*b*	-4.5 (-0.1)	-13.4 (-0.4)	-17.5 (-0.6)	*b*	*c*
Aluminum Remelt No. 2	1150	530	*b*	*b*	-120	-60	-73	*b*	*c*
Forge	1175	4440	+1.6	*b*	+9.7	-4.0	+2.4	*b*	*c*
Steel Reheat	1100	1455	-1.6	*b*	0	-22	+7.3	*b*	*c*
Steel Soaking Pit No. 1	925	2280	-1.5	*b*	-0.8	-5.4	+3.1	*b*	*c*
Steel Soaking Pit No. 2	1250	3460	-112 (-3.5)	-112 (-3.5)	*b*	-137[e] (-4.3)	*b*	-129 (-4.1)	-217 (-6.8)

[a]Positive values indicate surface deposits.

[b]Not included in this test.

[c]Not determined.

[d]Corrosion rate in mm/y.

[e]Corrosion rate for NC-430 coated with zircon was -112 m/s.

and because of cracking. The alumina and mullite exhibited no surface recession during exposure in aluminum remelt furnace No. 1.

MICROSTRUCTURAL VIEWS OF EXPOSED SURFACES

Typical microstructures of exposed sintered-α SiC (Hexoloy SA) are shown in Fig. 21. The cracks oriented approximately parallel to the surfaces of these specimens occurred while cutting the samples with a diamond-impregnated cutoff wheel. Grinding and polishing approximately 1 mm from the cut surface usually removes all cracks and proves that cracks of this type are not caused by exposure to the furnace environments. The specimen exposed to the aluminum remelt furnace had a very thin glass coating on the surface (Fig. 21a). The rougher surface of this specimen indicates more extensive corrosion compared to those in the other furnaces. This indication of corrosion is strongly supported by the decrease of diameter presented in Tables 5 and 6.

As compared to the other exposures, the Hexoloy SA exposed in steel soaking pit No. 2 showed extensive corrosion. Typical microstructures are in Fig. 22. The surfaces were covered with a slag coating that varied from zero to ~300 μm thick with the thinnest coating on the upstream side. Numerous metallic appearing inclusions were located throughout the slag coating and at the slag-SiC interface. As shown in Figs. 23 and 24, electron microprobe analysis identified iron as the major constituent in the inclusions dispersed in the slag, whereas the metallic inclusions at the slag-SiC interface contained iron and nickel. In addition, the electron microprobe found potassium in the silicate slag.

At the exposure temperature of this test the dissolved iron might have reacted with SiC in the manner described by other investigators,[9] producing Fe-Si alloys and gas by reactions of the type

$$Fe_2O_3 + 3SiC \rightarrow Fe_2Si_3 + 3CO \quad .$$

Fe-Si alloys containing 30 to 70 at. % Si would be partially molten at the exposure temperature except for pure, stoichiometric FeSi (m.p. 1410°C). Oxidation of the Fe-Si reaction product in the continually replenished

ORNL-PHOTO 0529-85

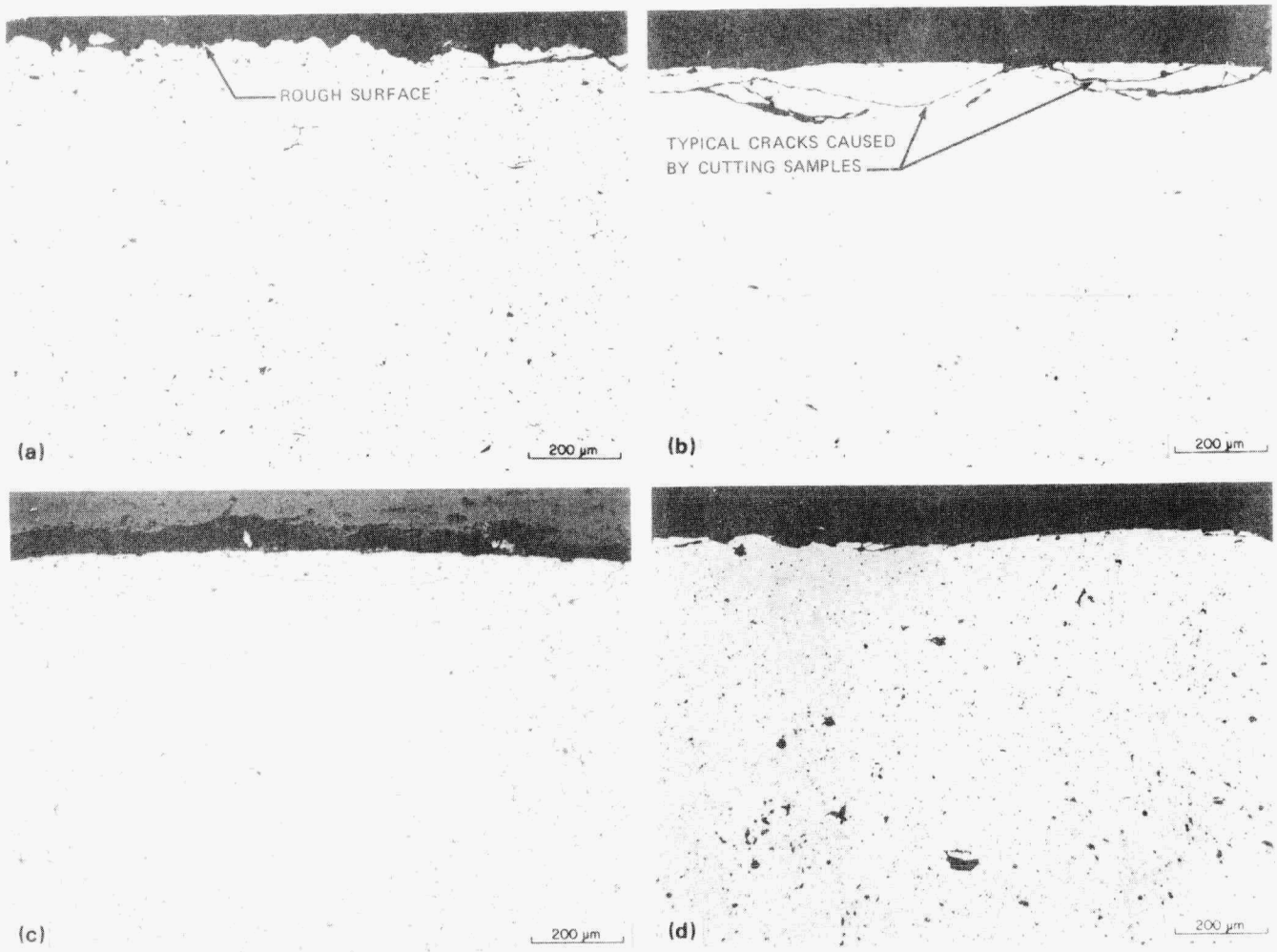

Fig. 21. Sintered-α SiC (Hexoloy SA) exposed to industrial furnace environments. (a) Aluminum remelt No. 1; (b) forge; (c) steel reheat; (d) steel soaking pit. As polished.

ORNL-PHOTO 0528-85

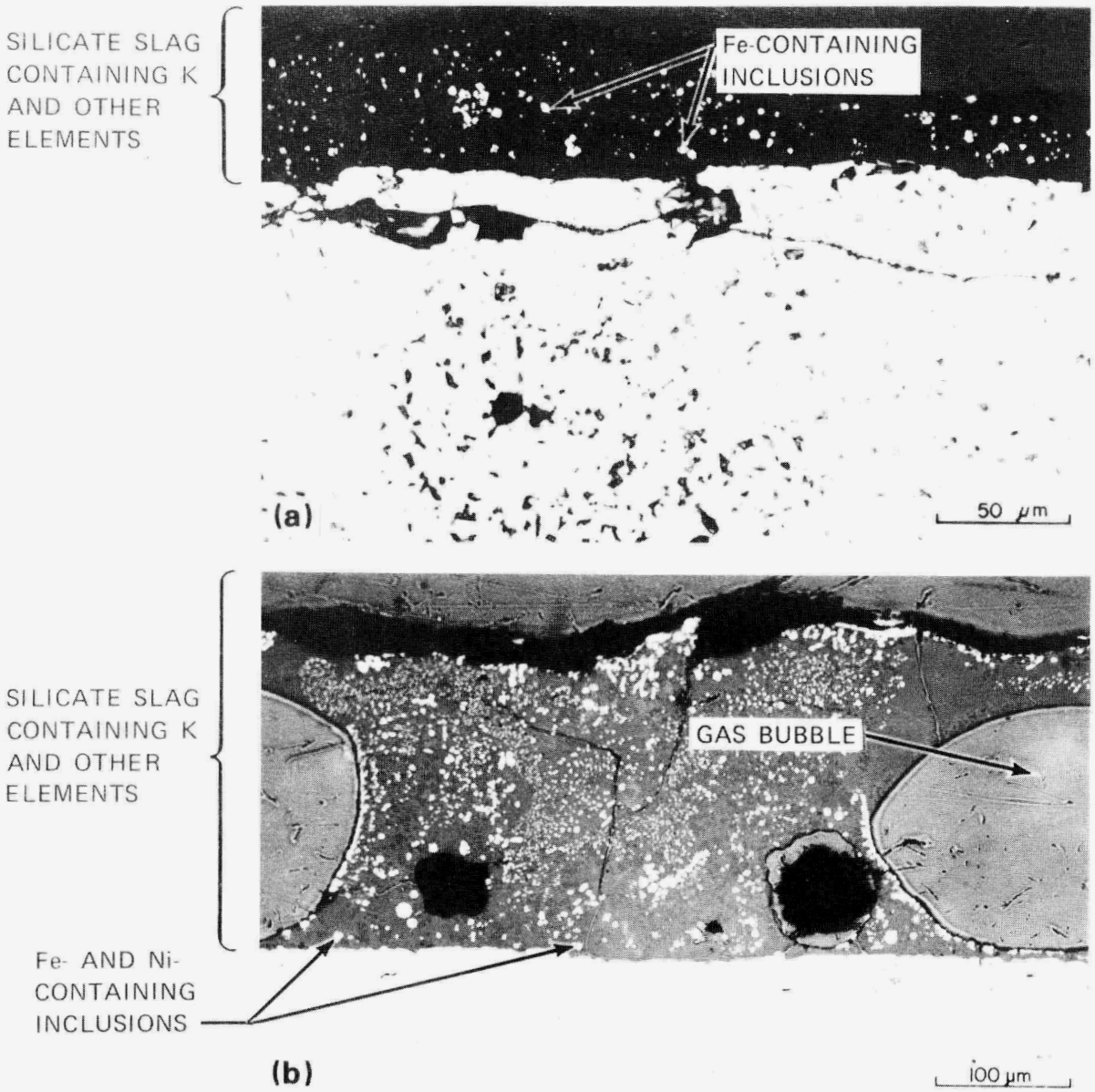

Fig. 22. Sintered-α SiC (Hexoloy SA) exposed in steel soaking pit No. 2. (a) Upstream region. (b) Down-stream region. As polished.

Y-197888

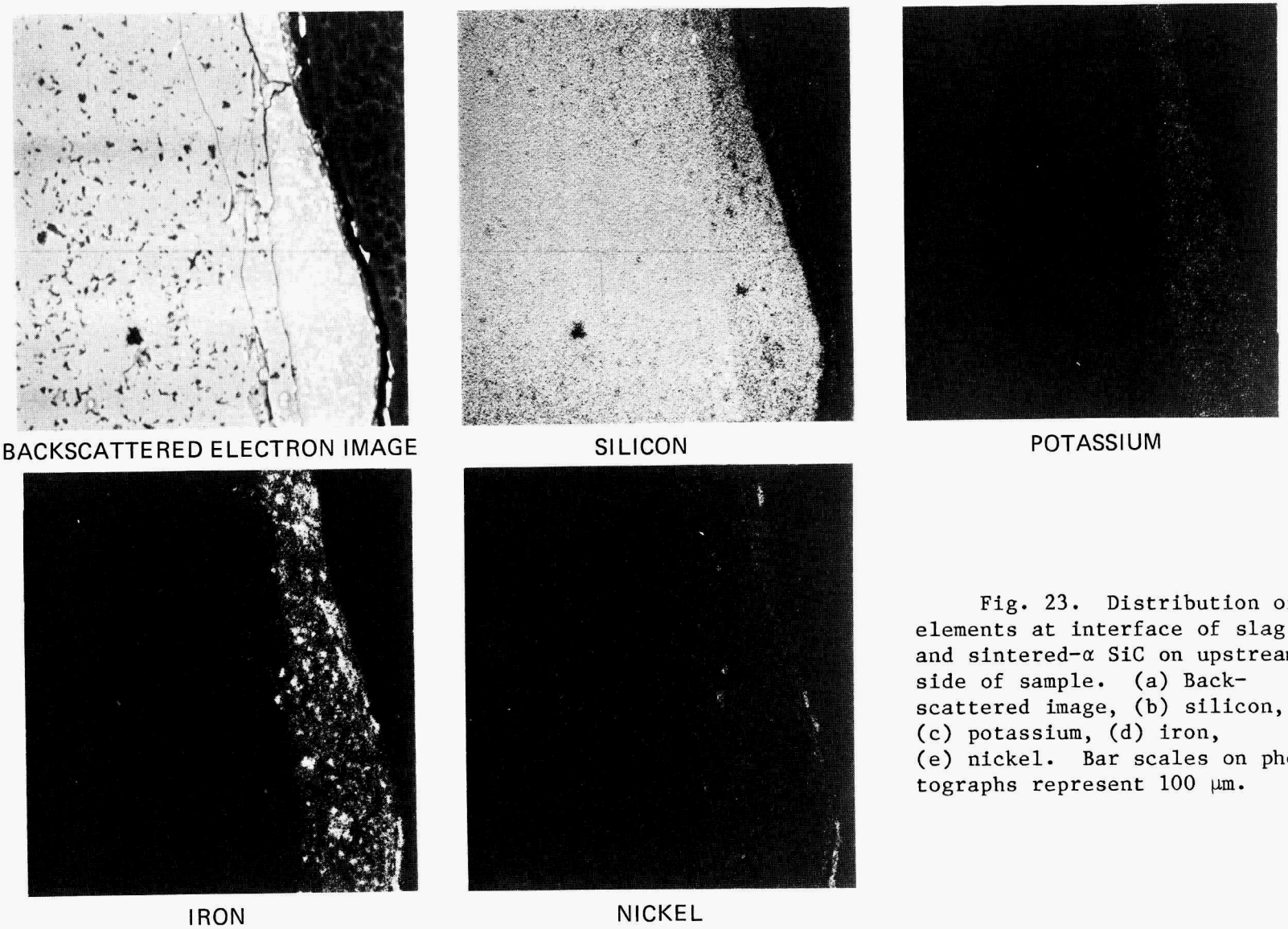

Fig. 23. Distribution of elements at interface of slag and sintered-α SiC on upstream side of sample. (a) Backscattered image, (b) silicon, (c) potassium, (d) iron, (e) nickel. Bar scales on photographs represent 100 μm.

Y-197886

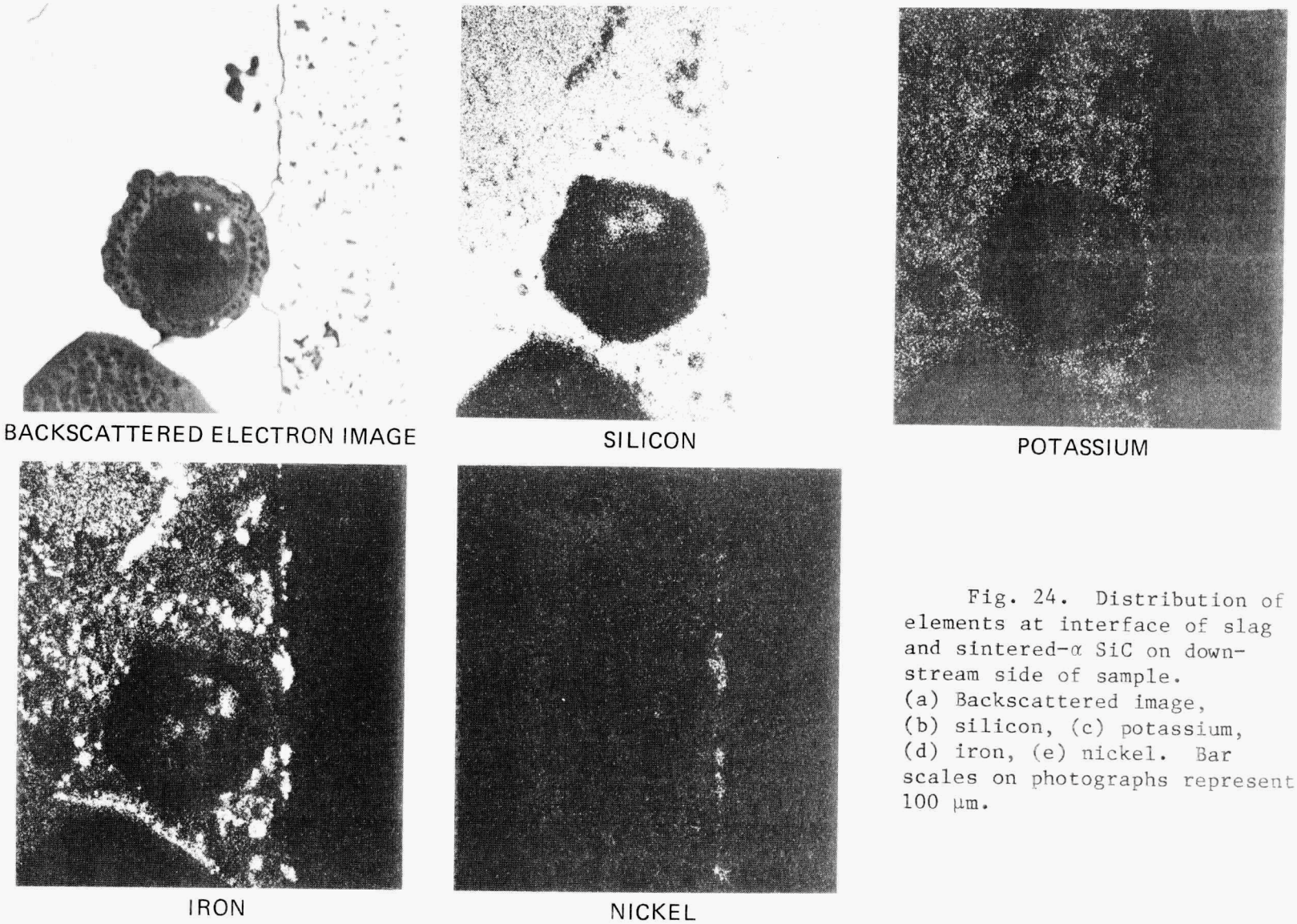

Fig. 24. Distribution of elements at interface of slag and sintered-α SiC on downstream side of sample. (a) Backscattered image, (b) silicon, (c) potassium, (d) iron, (e) nickel. Bar scales on photographs represent 100 μm.

slag would regenerate iron oxide and contribute silica to the slag. Voids in the slag might have been gas bubbles formed in reactions of the type mentioned above.

The porosity of recrystallized SiC (NC-400) is readily apparent in the microstructures in Fig. 25. The specimen exposed to aluminum remelt No. 2 had a relatively thick glass coating on the surface (Fig. 25a). Rounded surfaces of material in contact with the glass indicates that corrosion had occurred, as was revealed by changes in diameter presented in Tables 5 and 6. Penetration of glass into some pores is shown in Fig. 25b. The glass coated the surfaces of the pores, which were subsequently filled with epoxy during ceramographic sample preparation. A different coating, probably an oxide, is apparent on surfaces of pores in the other specimens.

Figure 26 shows microstructures of recrystallized SiC coated with SiC (NC-400/CVD SiC). This material had rough surfaces in the as-fabricated conditon; therefore, the surface roughness does not necessarily indicate the result of corrosion. There is no evidence of catastrophic corrosion in any of the specimens. The coating, which is similar to Hexoloy SA in purity and density, might have had similar surface recession; however, recession of these specimens was not measured. No other evidence of degradation of the coating or separation of the coating from the NC-400 substrates was observed except for slag penetration into the pores of the specimen exposed in aluminum remelt No. 1.

Typical microstructures of the siliconized SiC (NC-430) and reaction sintered SiC (SC-X) are shown in Figs. 27 and 28. Although diameter measurements indicated significant surface recession in specimens exposed to aluminum remelt furnace atmospheres, corrosion of these materials was not revealed as severe general attack or as selective attack on the silicon phase. The only indication of attack is slightly rougher surfaces (Figs. 27a, 27b, 28a and 28b). If the silicon phase were selectively attacked, the surface area of SiC exposed to the corroding species would increase, and corrosion might accelerate. Electron microprobe analyses, in agreement with previously discussed chemical analyses, indicated the presence of Al, Ca, Fe, K, Na, Si, and Zn in the glassy deposits on specimens exposed to aluminum remelt furnace atmospheres. No evidence for penetration of these or other elements into the silicon phase was detected.

ORNL-PHOTO 0527-85

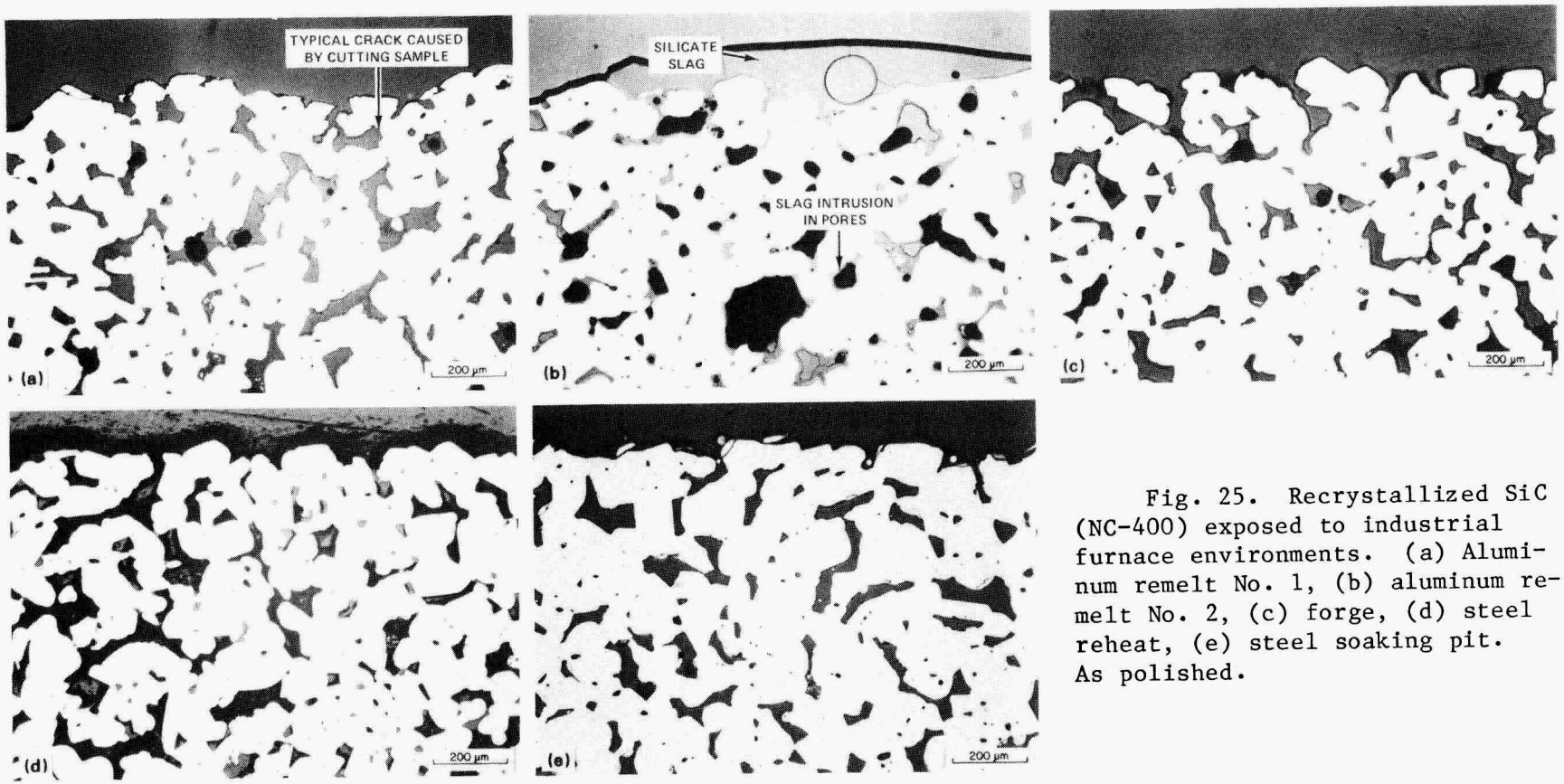

Fig. 25. Recrystallized SiC (NC-400) exposed to industrial furnace environments. (a) Aluminum remelt No. 1, (b) aluminum remelt No. 2, (c) forge, (d) steel reheat, (e) steel soaking pit. As polished.

ORNL-PHOTO 0526-85

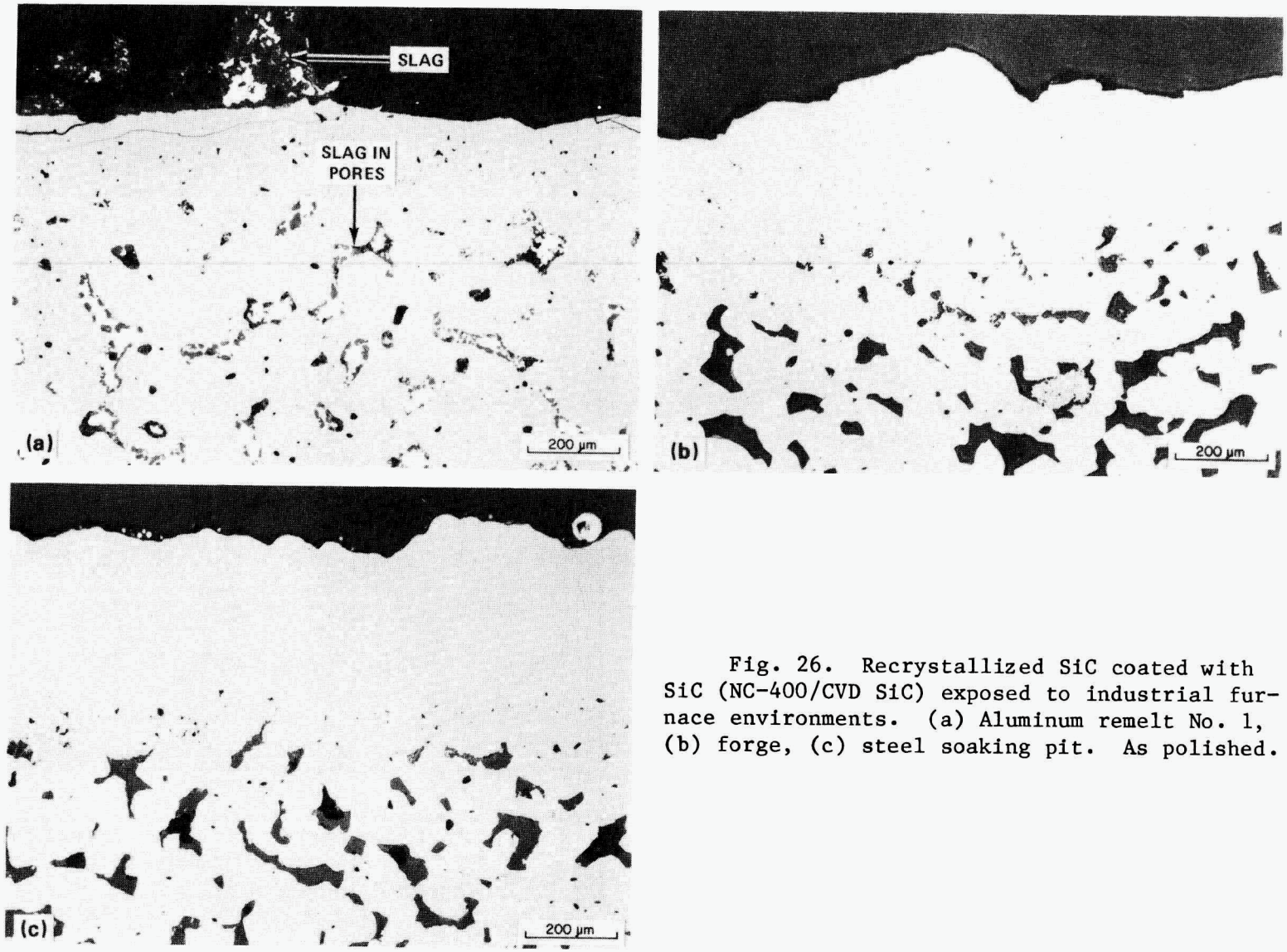

Fig. 26. Recrystallized SiC coated with SiC (NC-400/CVD SiC) exposed to industrial furnace environments. (a) Aluminum remelt No. 1, (b) forge, (c) steel soaking pit. As polished.

ORNL-PHOTO 0524-85

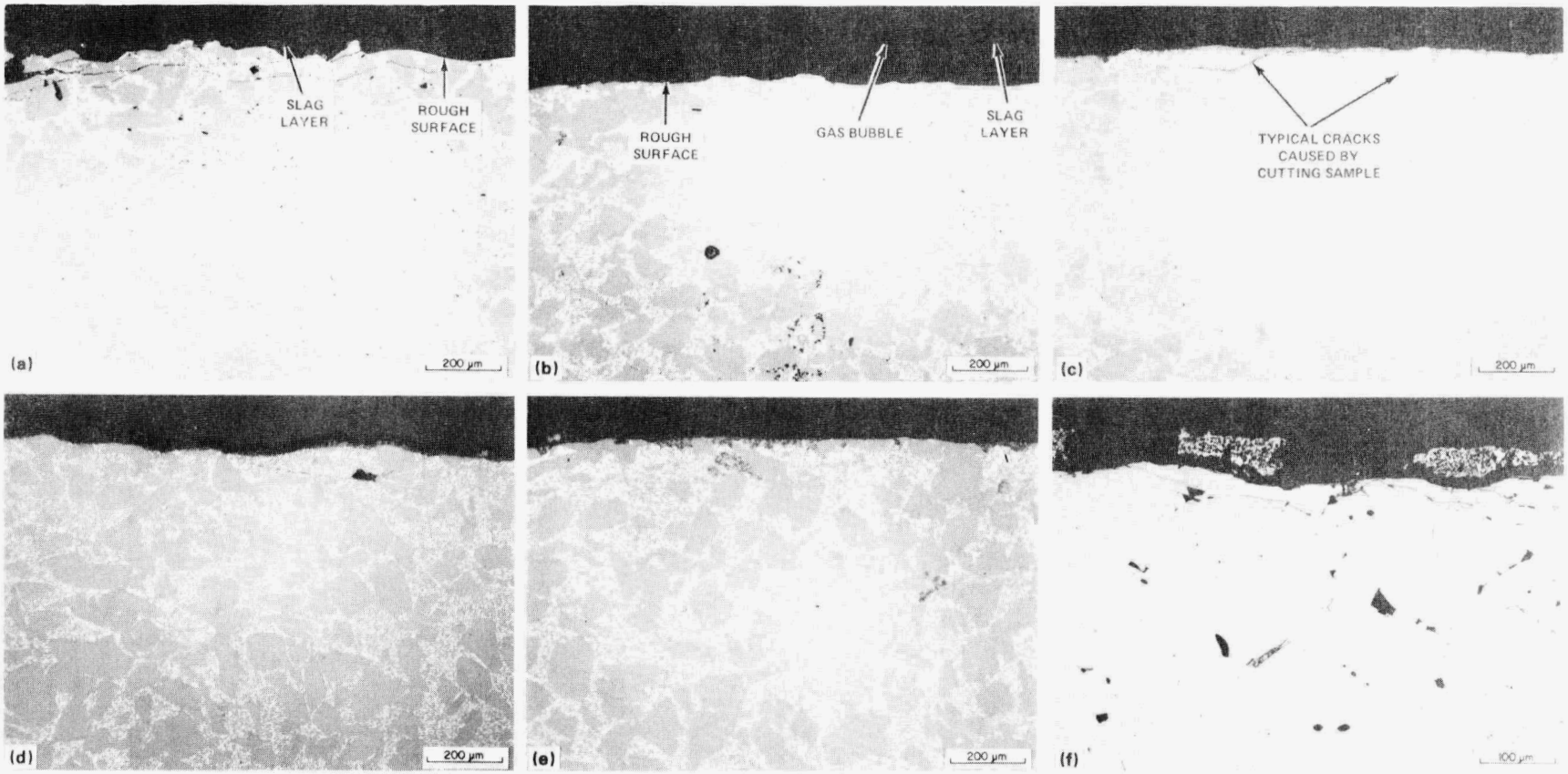

Fig. 27. Siliconized SiC (NC-430) exposed to industrial furnace environments. (a) Aluminum remelt No. 1, (b) aluminum remelt No. 2, (c) forge, (d) steel reheat, (e) steel soaking pit No. 1, (f) steel soaking pit No. 2. As polished.

ORNL-PHOTO 0523-85

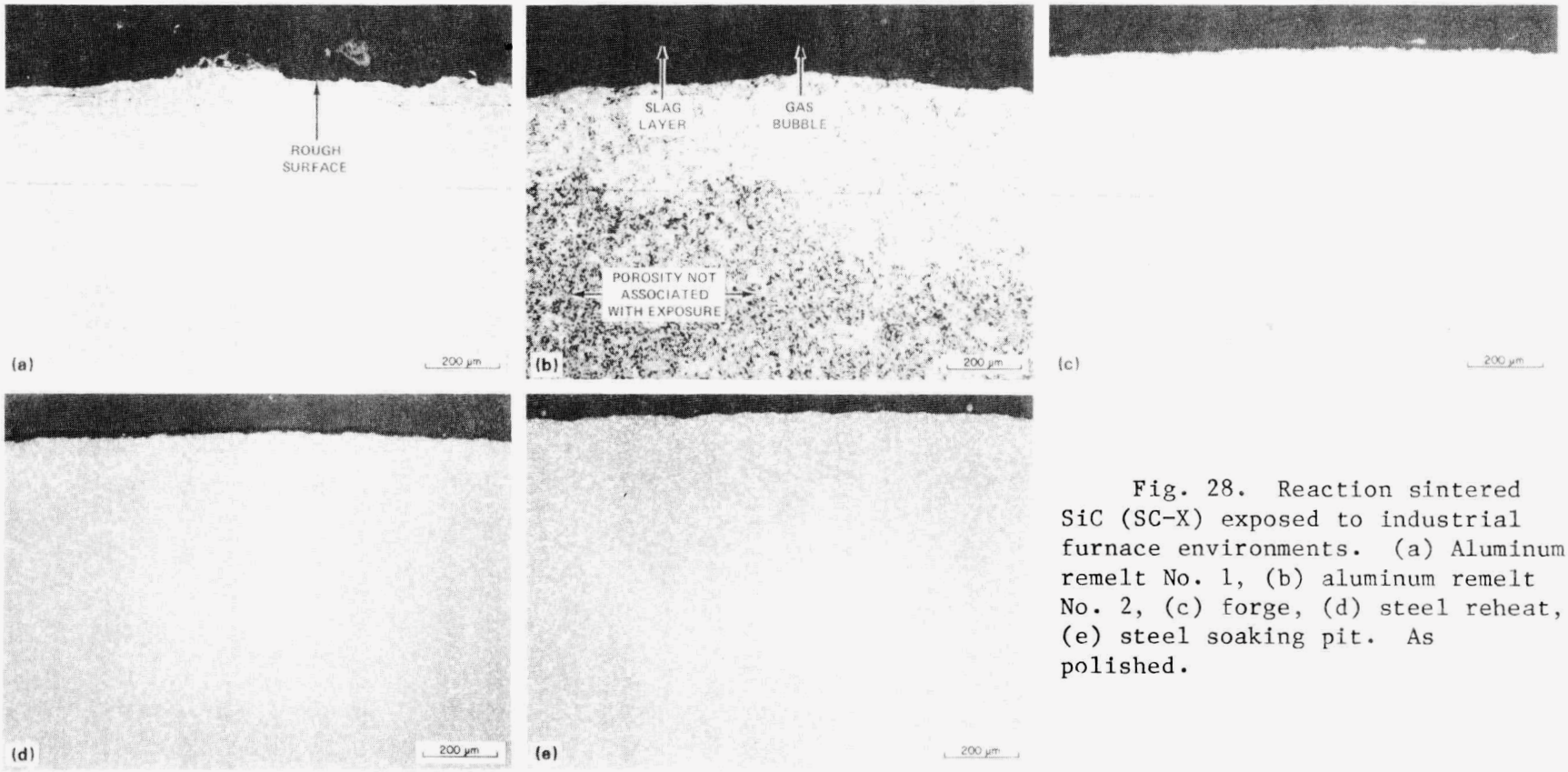

Fig. 28. Reaction sintered SiC (SC-X) exposed to industrial furnace environments. (a) Aluminum remelt No. 1, (b) aluminum remelt No. 2, (c) forge, (d) steel reheat, (e) steel soaking pit. As polished.

The siliconized SiC (NC-430) exposed in steel soaking pit No. 2 also showed significant surface recession during exposure. As previously discussed, the recession is believed to be a result of a corrosion/erosion mechanism where the slag coating was actually able to flow to the downstream side of the tube, thus exposing a "new" surface. A typical area on the upstream side with no slag coating is shown in Fig. 27f. The slag coatings that were present contained metallic appearing inclusions and gas bubbles similar to those observed with the sintered-α SiC.

Also included in steel soaking pit No. 2 was a tube of NC-430 coated on the upstream side with a thin layer of zircon (~70 μm thick). The intention of the coating was to provide a thermal barrier on the hot side and thus reduce the thermal stresses during exposure. Examination after exposure revealed no evidence of the zircon coating as shown by comparison of Figs. 29a and b. As mentioned in Table 6, the corrosion rate was lower for the coated specimen (-112 vs -137 pm/s for the uncoated specimen); however, the ceramographic examination provided no explanation for the difference. We suspect that the zircon coat did provide some protection for a short period of time, after which corrosion proceeded like that for the uncoated NC-430. The absence of free Si was also observed in the original, unexposed NC-430; therefore, the absence of free Si in the exposed NC-430 was not caused by corrosion.

Figure 28b reveals considerable porosity in the SC-X material. This porosity apparently formed during fabrication as the result of incomplete filling of the skeletal SiC structure by silicon. The SC-X specimens generally contained less porosity than that shown in Fig. 28b.

As previously discussed, the Si_3N_4-bonded SiC ceramics cracked extensively during the exposure tests. Figures 30 and 31 show typical microstructures of these materials. In addition to cracking, surface recession evidently occurred in specimens exposed to aluminum remelt and steel soaking pit No. 2 furnaces. Figures 30b, 30e, and 31a show glassy deposits on these materials. Large bubbles in the glassy deposit (Fig. 30b) originate at the bonding phase, which appears to be recessed leaving SiC particles in relief. Although bubbles are not apparent in the glassy deposit in Figs. 30a and 31a, SiC particles are isolated in the glass, suggesting that the bonding phase has dissolved. Similar observations were made in the samples from steel soaking pit No. 2 with

ORNL-PHOTO 0816-85

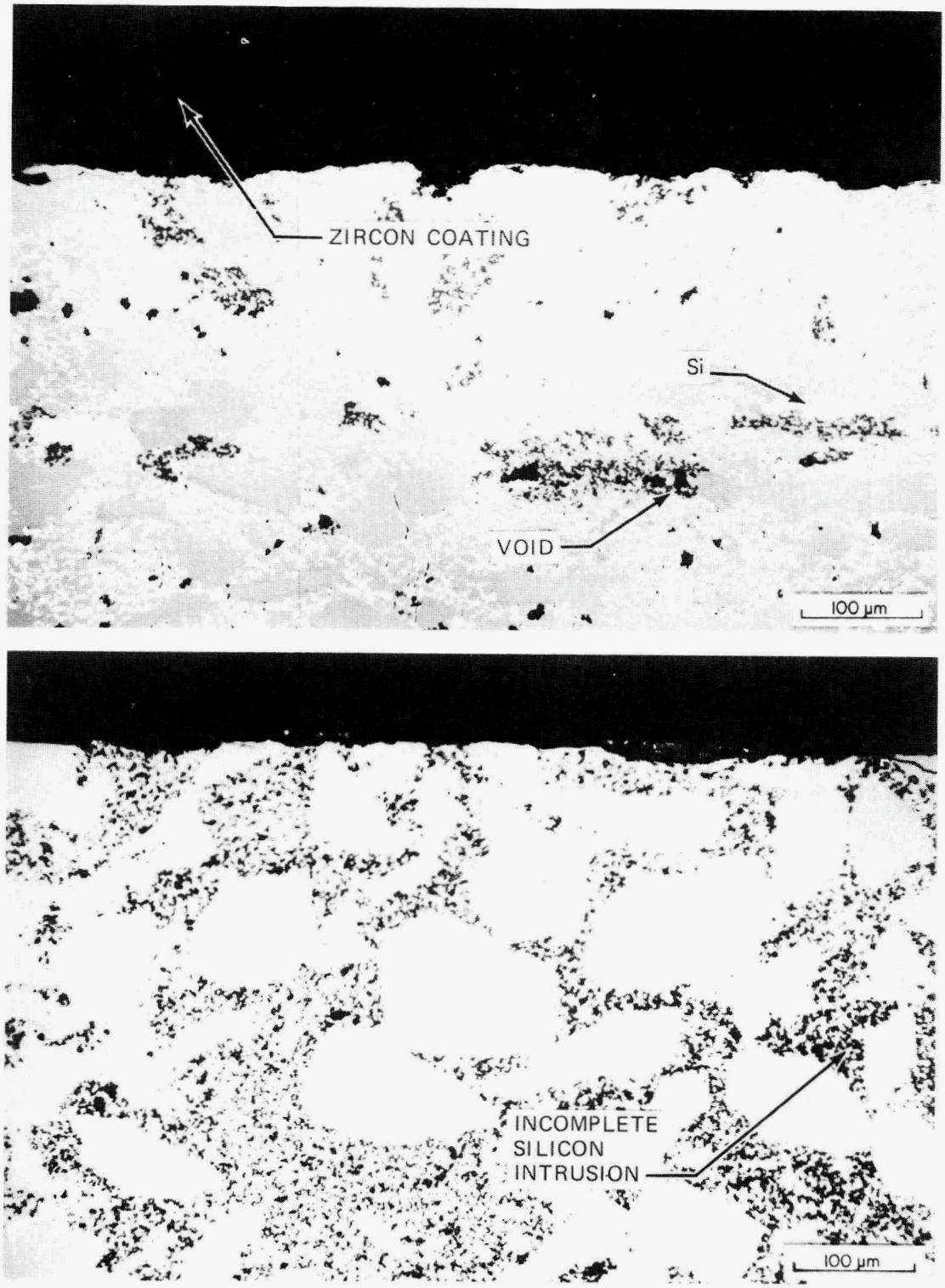

Fig. 29. Siliconized SiC (NC-430) with a zircon coating. (a) Unexposed, showing zircon coating. (b) After exposure in steel soaking pit No. 2.

ORNL-PHOTO 0522-85

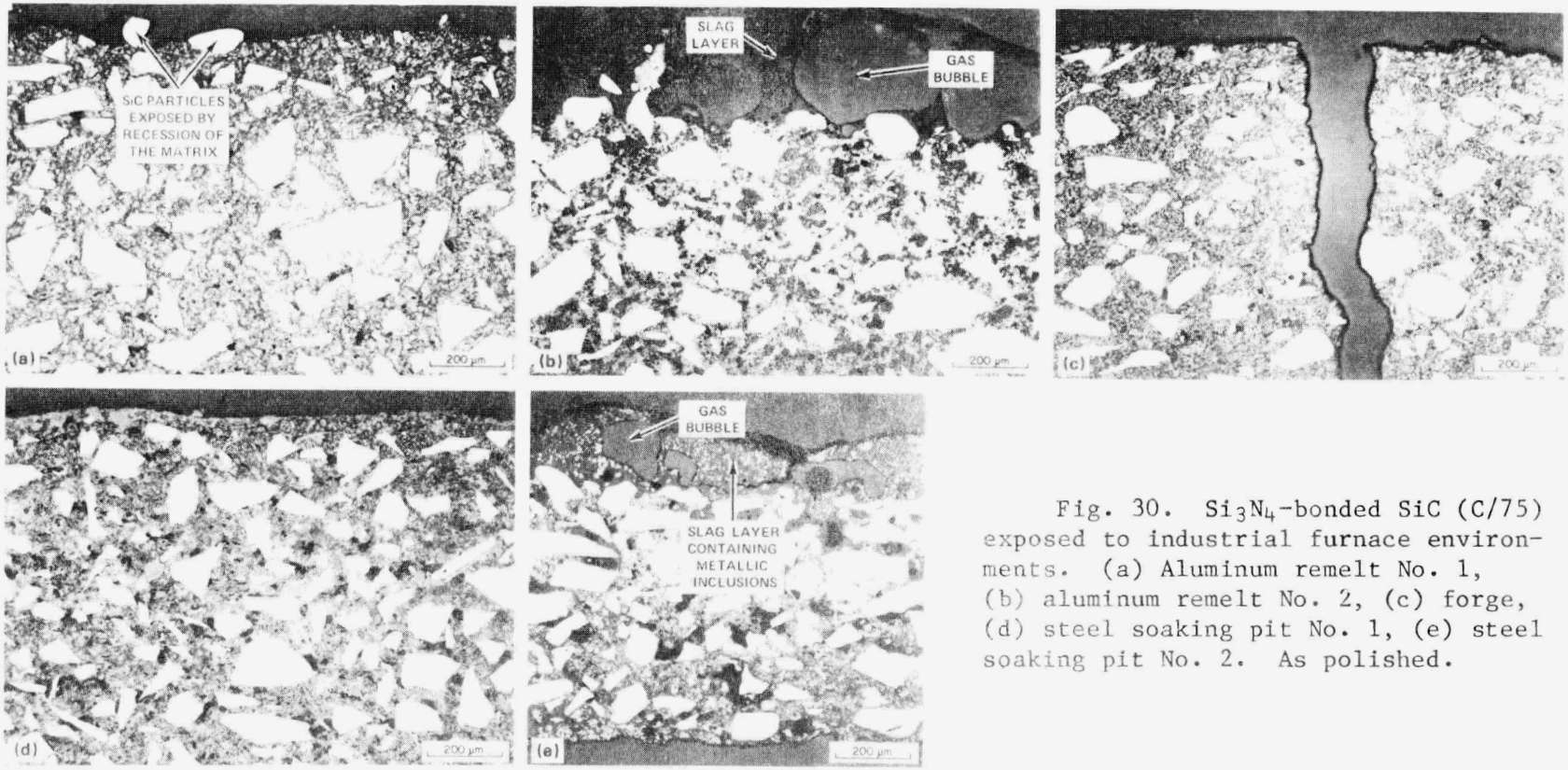

Fig. 30. Si_3N_4-bonded SiC (C/75) exposed to industrial furnace environments. (a) Aluminum remelt No. 1, (b) aluminum remelt No. 2, (c) forge, (d) steel soaking pit No. 1, (e) steel soaking pit No. 2. As polished.

ORNL-PHOTO 0521-85

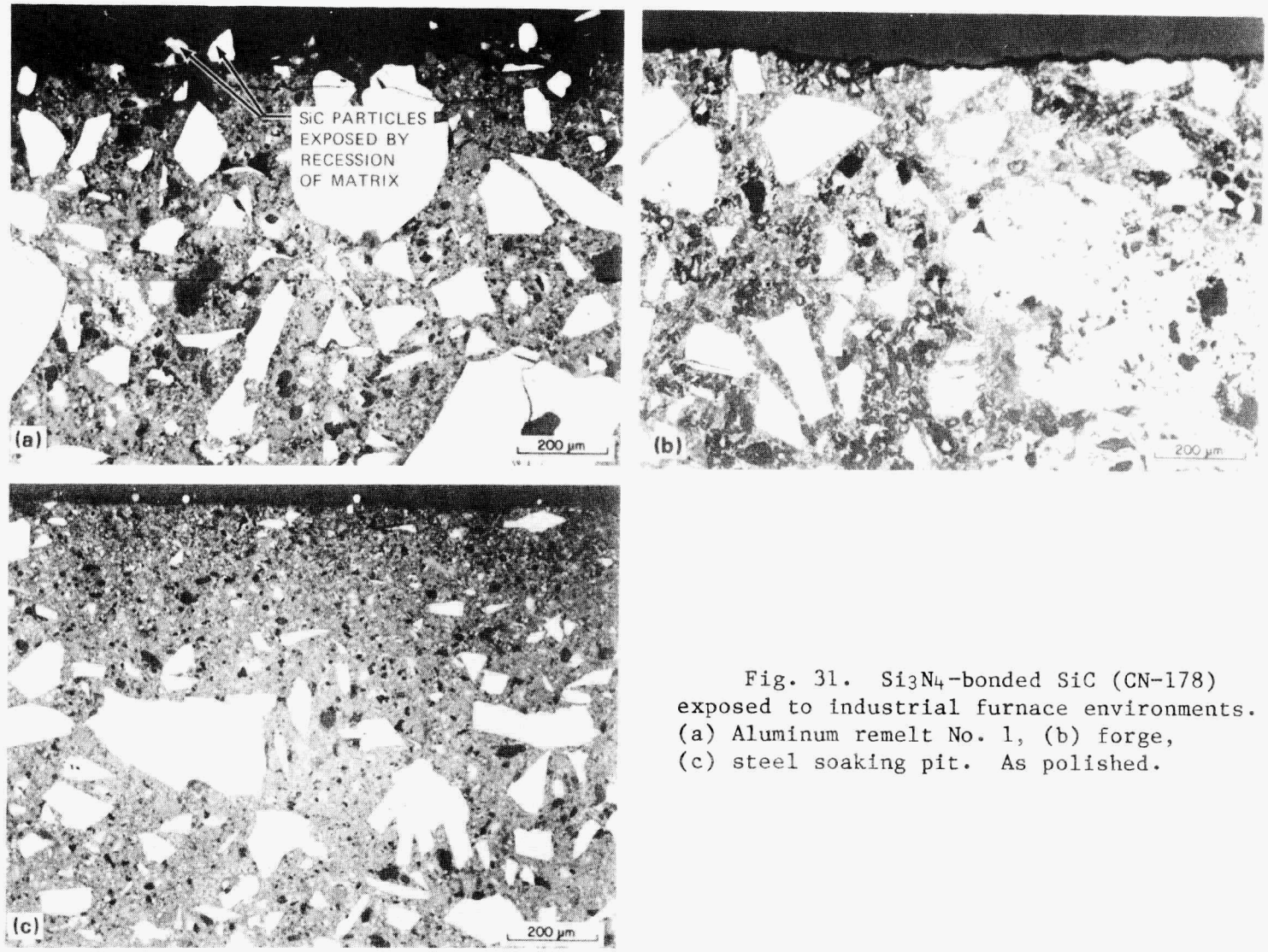

Fig. 31. Si_3N_4-bonded SiC (CN-178) exposed to industrial furnace environments. (a) Aluminum remelt No. 1, (b) forge, (c) steel soaking pit. As polished.

the addition that the slag coatings also contained metallic appearing inclusions (Fig. 30e). Significant corrosion of the bonding phase did not occur in specimens exposed to the steel reheat furnace No. 1; however, cracks of the type shown in Fig. 30c occurred frequently. The indicated corrosion in aluminum remelt and steel soaking pit No. 2 furnaces and the extensive cracking that occurred in all furnaces strongly suggest that these Si_3N_4-bonded SiC ceramics are not suitable for heat exchanger tubes or other applications requiring leak tightness and strength at elevated temperatures.

A sample of the nitride bonded SiC exposed in steel soaking pit No. 2 was examined with the electron microprobe. Those results are summarized in Fig. 32. As shown, considerable iron and nickel was found in the metallic appearing inclusions dispersed throughout the slag coating and at the slag-SiC interface. In addition, iron and nickel were observed extending well past the SiC particles in the nitride-bonded matrix. Enhanced corrosion in these areas, leaving the SiC particles in relief, is believed to be the cause of the poor performance of these materials in the exposure test.

The exposure test in steel soaking pit No. 2 also contained another siliconized SiC (KT) and Sintride (SSIC), which were not used in the other tests. The KT-SiC was similar in appearance ceramographically to the NC-430 samples previously discussed (Fig. 33), which was not unexpected because their corrosion rates were similar. Gas bubbles and metallic appearing inclusions were observed throughout the slag coatings.

A typical microstructure of the Sintride specimen exposed in steel soaking pit No. 2 is presented in Fig. 34. Again the slag coatings contain gas bubbles and dispersed metallic appearing inclusions. In addition, some metallic appearing inclusions at the slag-SiC interface were observed, which were similar to those found with the α-SiC (Hexoloy SA).

Microstructures of the two oxide ceramics exposed to the aluminum remelt furnace No. 1 environment are shown in Fig. 35. The alumina exhibits a reaction layer at the surface, which was probably responsible for the slight diameter increase determined for this specimen. Mullite, which had no measurable change in diameter, appears to be unaffected by the exposure.

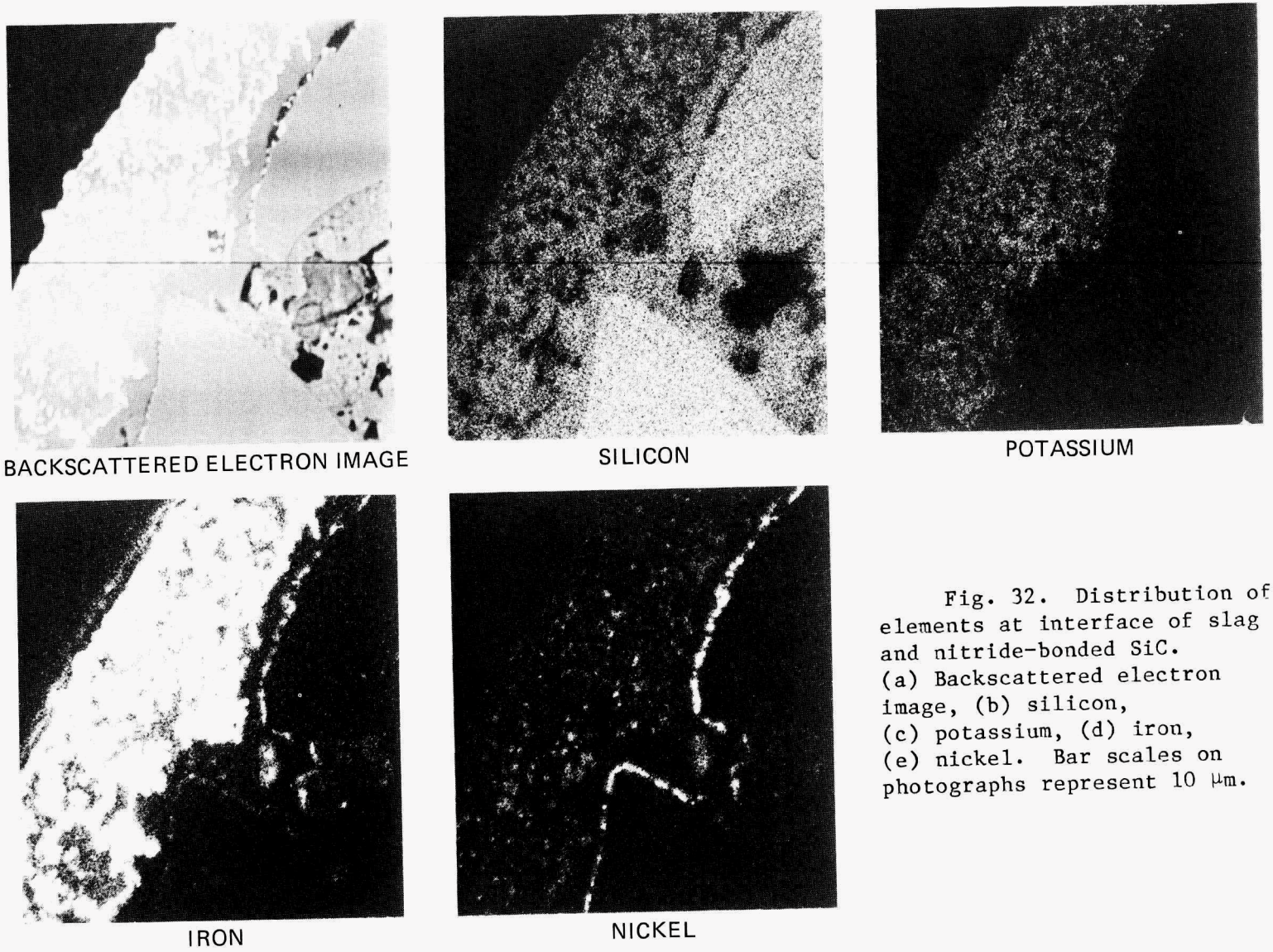

Fig. 32. Distribution of elements at interface of slag and nitride-bonded SiC. (a) Backscattered electron image, (b) silicon, (c) potassium, (d) iron, (e) nickel. Bar scales on photographs represent 10 μm.

ORNL-PHOTO 0520-85

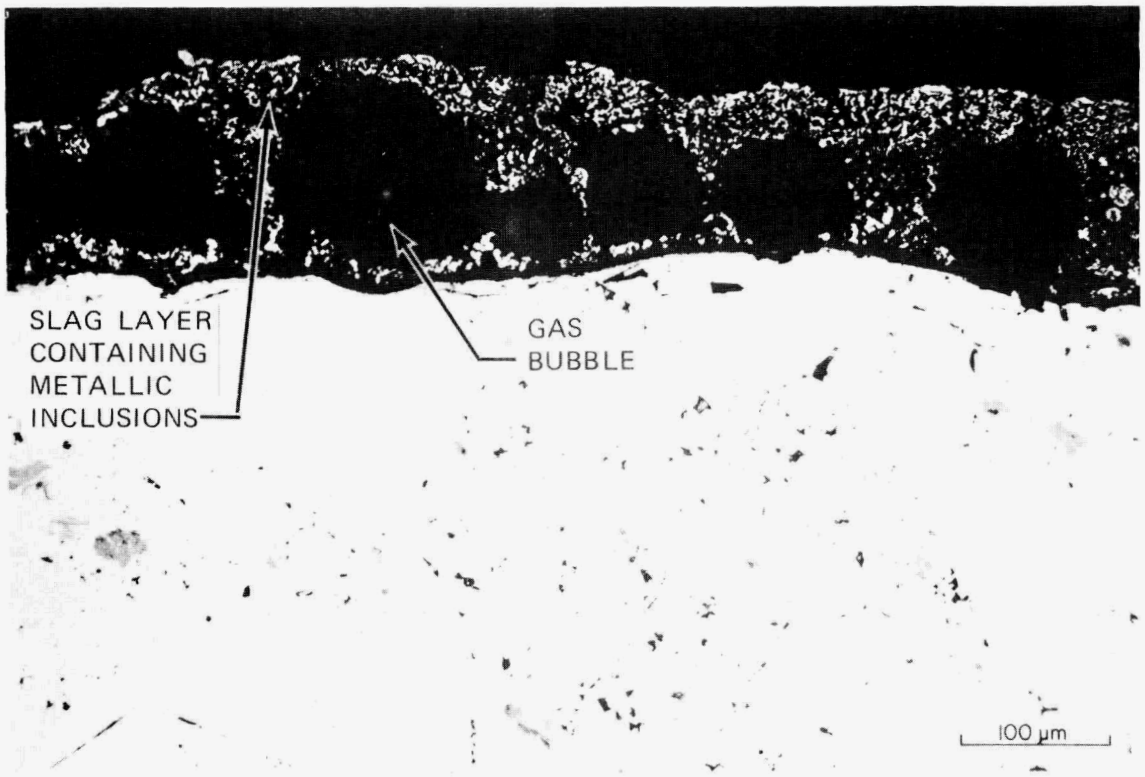

Fig. 33. Siliconized SiC (KT) exposed in steel soaking pit No. 2. As polished.

ORNL-PHOTO 0815-85

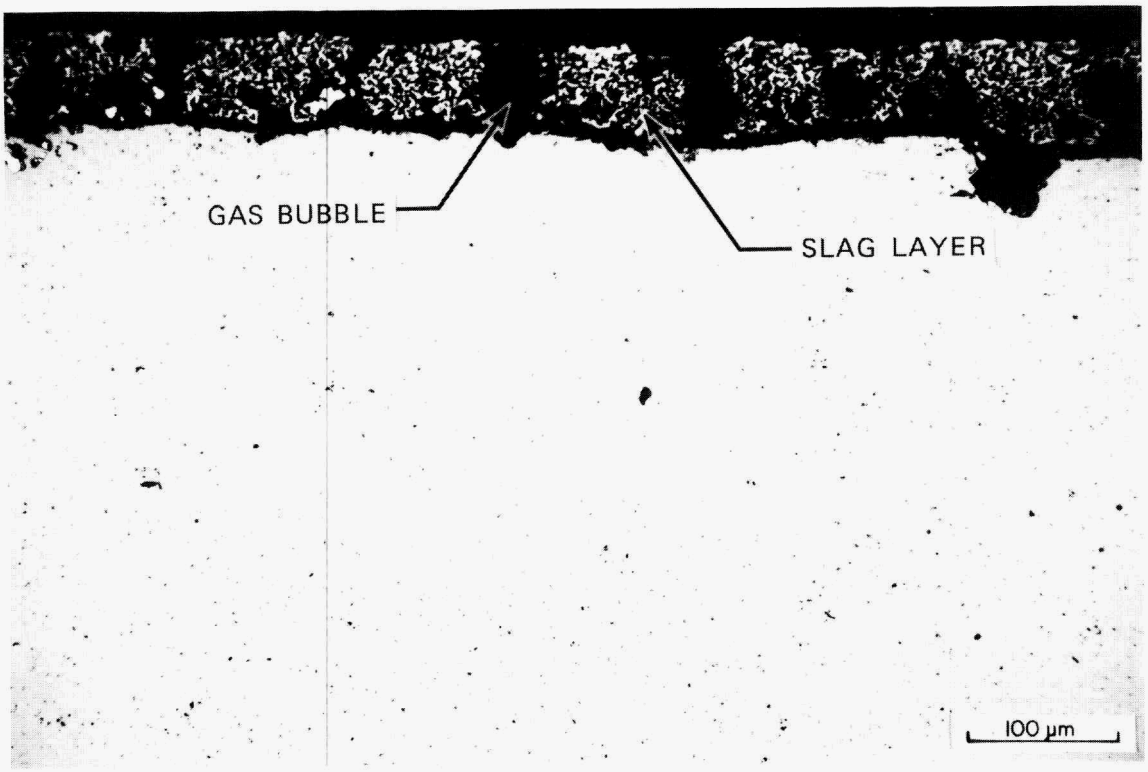

Fig. 34. Sintride exposed in steel soaking pit No. 2. As polished.

ORNL-PHOTO 0519-85

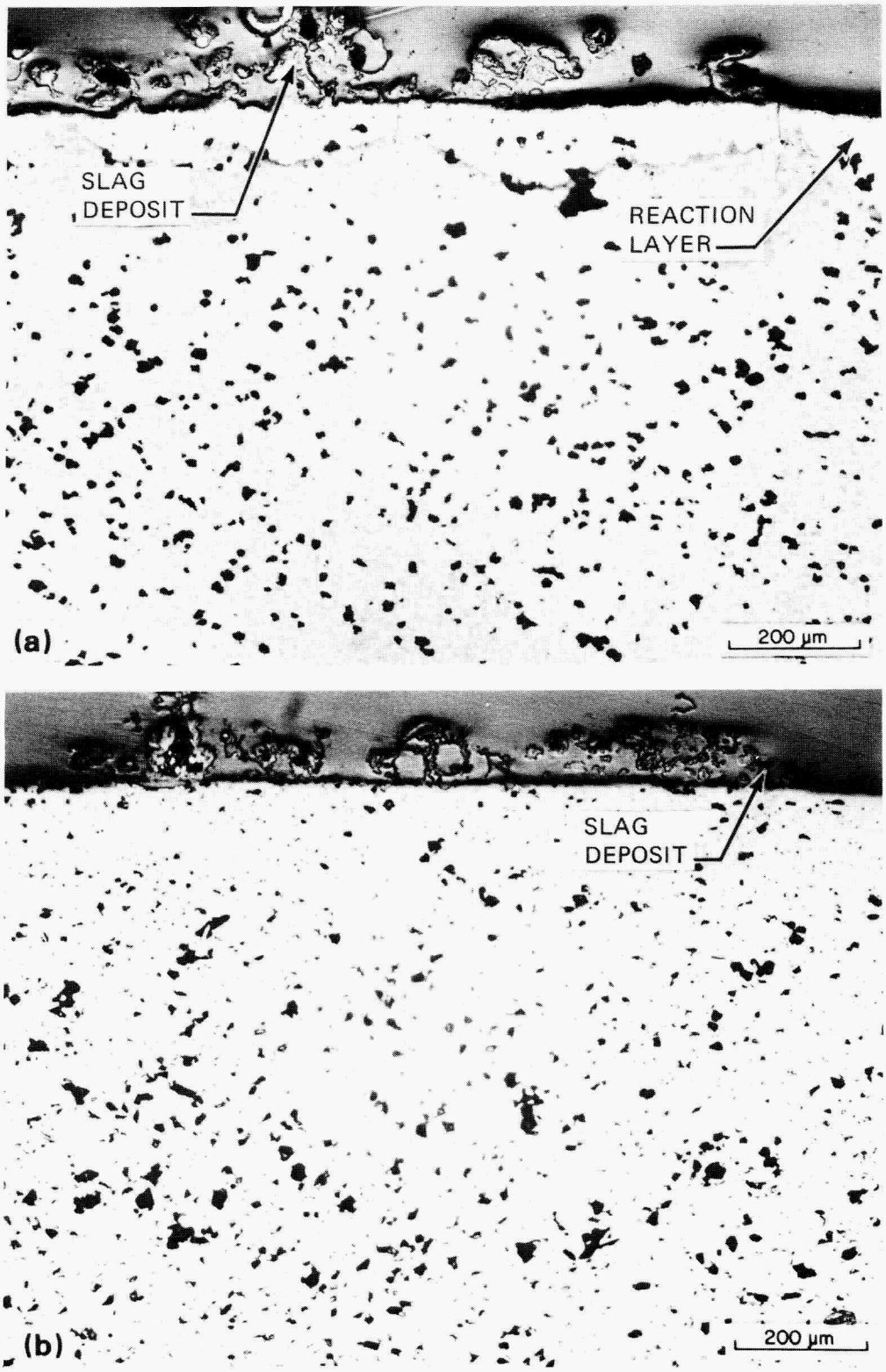

Fig. 35. Oxide ceramics exposed to aluminum remelt furnace No. 1 environment. (a) Alumina (AD-998); (b) mullite. As polished.

FLEXURE STRENGTH

The flexure strengths of Hexoloy SA and NC-430 were determined in order to assess degradation of mechanical properties caused by exposure to the furnace environments. C-ring specimens cut from tubes provided a convenient method of subjecting the outer surfaces to tensile stresses. The outer surfaces of the specimens (the original outer, exposed surfaces of the tubes) were not deliberately treated or altered during specimen preparation or testing. In the case of specimens that had been exposed to aluminum remelt furnace No. 1 the loosely adhering deposits mostly detached during handling; however, the thin glass coating remained intact. Tubes were cut into 5-mm-wide rings using a cutoff wheel impregnated with 75 μm diamonds. C-rings were made by cutting approximately 5 mm long arcs from the rings. The final thickness of the rings was obtained by grinding both sides with 75 μm diamond abrasive. The outer edges of specimens were beveled with a 30 μm diamond lapping wheel.

The specimens were loaded so that a tensile stress was applied to the outer surface at a point opposite the open part of the ring. Specimens were heated to 1100°C in air, then the loading ram was advanced at 8.5 μm/s (0.02 in./min) until fracture occurred. The fracture stress (σ) was calculated from the load and specimen dimensions using the following equation applicable to the C-ring geometry as described by Ferber and Tennery.[10]

$$\sigma = \frac{P}{(r_o - r_i)w} \quad 1 + \frac{r_o + r_i}{2\ r_o} \quad \frac{R - r_o}{\bar{r} - R} ,$$

where

P = load,

r_o = outer radius,

r_i = inner radius,

w = width,

$\bar{r}$ = $(r_o + r_i)/2$,

R = $(r_o - r_i)/\ln (r_o/r_i)$.

The mean fracture strength for Hexoloy SA varied from a maximum value of 238 MPa for specimens exposed to the steel forge furnace to a minimum of 204 MPa for specimens exposed to aluminum remelt No. 1 (Table 7). These results indicate that the strength of Hexoloy SA was affected by the exposures. Specimens with the lowest strength had the largest surface recession (Table 5) and the roughest surface. In the case of NC-430 the lowest strength occurred in specimens exposed in steel soaking pit No. 1 (least surface recession); however, the next lowest strength occurred in specimens exposed in aluminum remelt No. 1 (maximum surface recession). These results suggest that fracture strength is affected by thermal exposure history in addition to corrosion.

Table 7. C-ring fracture strength of Hexoloy SA and NC-430 at 1100°C after exposure to industrial furnace environments

Furnace	Mean fracture strength, MPa	
	Hexoloy SA	NC-430
Aluminum remelt No. 1	204 (12)[a]	184 (12)
Aluminum remelt No. 2		220 (6)
Steel forge	238 (9)	
Steel reheat	231 (12)	325 (12)
Steel soaking pit No. 1	233 (11)	162 (12)

[a]Indicates number of specimens tested.

DISCUSSION

The principal results disclosed by the present work are associated with materials exposed to aluminum remelt furnaces. In that environment the SiC ceramics had significant surface recessions, the siliconized and reaction sintered types corroding more than the high purity types. In addition, sintered-α SiC exposed to different furnace environments exhibited a range of average fracture strengths, the weakest being that exposed to aluminum remelt furnace No. 1. These results, therefore, show

that significant degradation of SiC ceramics will occur in certain furnace environments.

The corrosion in the aluminum remelt furnaces experienced by SiC ceramics project to annual recession rates ranging from approximately 0.5 to 1 mm/y depending on type of material. Another study of corrosion of SiC ceramics in an aluminum remelt furnace revealed even higher recession rates.[11] In that study projected recession rates for materials exposed at about 1100°C ranged from about 3 mm/y for sintered-α SiC to 10 mm/y for siliconized SiC (NC-430), that is, about a factor of ten higher than determined in the present study. Several factors might be responsible for this large difference in the corrosion rates. Exposure times and temperatures are best estimates in both cases. The frequency and severity of thermal cycling is not well known. The composition of flue gases and particulates might be substantially different in the two cases. The chloride content, for example, of the slag on specimens in aluminum remelt furnace No. 1 was less than 100 ppm, but the solids in the flue gases in the work of Russell et al.[11] included halide compounds containing 47 to 58% Cl and 0.05 to 0.22% F. In fact Russell et al. suggest that the dominant corrosion mechanism in their work was reaction of SiC, Si, and SiO_2 with halide species in the flue gases resulting in formation of volatile silicon halides. Although unproven, this hypothesis seems to be the most logical explanation for the observed corrosion.

In at least one other study, however, SiC was resistant to attack by NaCl (ref. 12). Reaction sintered and hot pressed SiC were immersed in molten NaCl at 1000°C for 1 h in air. The only result was a slight weight gain, which was attributed to oxidation of SiC to form SiO_2 by oxygen dissolved in the molten NaCl. The investigators suggest that the resulting SiO_2 layer was stable because the oxygen ion activity of the melt was too low for dissolution of SiO_2 as a silicate radical. The same study revealed considerable weight losses when SiC ceramics were exposed to molten Na_2SO_4 and Na_2SO_4-NaCl eutectic.

Combustion atmospheres are often quite complex. Specimens exposed to these atmospheres reveal the net result of attack by some of the species, but the role of various species is not readily determined. Additional work is needed which would allow the role of various suspected corrodants

to be determined individually and in combination. Then, if the constituents of the flue gases in a particular furnace are known, the behavior of materials exposed to the furnace environment might be predicted.

The high corrosion rates observed in steel soaking pit No. 2 are attributable to their position in the flue during the test. These samples were subjected to temperatures up to 1250°C, high velocity exhaust gases and particulates from the furnace environment. Actual placement of a recuperator would be further down the flue where the temperature, exhaust gas velocity, and amount of particulates would all be substantially lower. Consequently, we would expect the corrosion rates to be substantially lower also.

The C-ring flexure strengths obtained in this work (Table 7) are considerably less than the flexural strengths reported by the manufacturers,[13,14] which are 450 MPa at 1200°C for Hexoloy SA and 275 MPa at 1100°C for NC-430. The manufacturer's flexural strength, however, was obtained under conditions designed to yield the highest strength with the least amount of variation. Test specimens were precisely machined bend bars with finely ground surfaces, which were subjected to three- or four-point loading until fracture occurred. In the present work C-rings were more easily prepared than bend bars from the tubular specimens. In addition, the tensile surfaces of the specimens, as previously mentioned, were not specially prepared prior to testing. Instead, all tensile surfaces were in the exposed condition. These surfaces undoubtedly contained relatively large flaws of the type that initiate cracks under tensile stresses, thereby resulting in lower average fracture strengths than would be obtained on specially prepared specimens. The number of specimens tested in each group was insufficient to determine accurately characteristic stresses and Weibull moduli.

More important than the difference in flexural strength between C-rings tested in the present work and the published strength of sintered-α SiC is the apparent weakening of material exposed to certain furnace environments. The average C-ring fracture strength of sintered-α SiC was lowest for specimens exposed to aluminum remelt furnace No. 1, while that of NC-430 was lowest for specimens exposed in steel soaking pit No. 1. Because substantially more surface recession occurred in the former as

shown in Table 5, the amount of corrosion apparently is not the only factor affecting strength. Attack at grain boundaries or at impurity sites might be important. Also, the exposure conditions might cause microcracking, which would affect the mechanical properties.

Although the reasons for different strengths is not clear, the fact that weakening occurs is important. Corrosion, which decreases the load-bearing ability of the material, could be accommodated by using sufficiently thick sections to attain desired lifetime. Continuing degradation of strength with increasing exposure, however, would be more serious. The present work unfortunately does not indicate if strength degradation occurred early in the exposure or occurred gradually.

SUMMARY

Candidate ceramic materials have been exposed to six industrial furnace atmospheres. The materials were sintered-α SiC (Hexoloy SA), Sintride, recrystallized SiC (NC-400), siliconized or reaction sintered SiC (NC-430, SC-X, and KT), CVD SiC-coated SiC (NC-400/CVD SiC), Si_3N_4-bonded SiC (C/75 and CN-178), alumina (AD-998), and mullite. Tubes or bars of these materials were exposed to the environments of two aluminum remelt furnaces, a forge furnace, a steel reheat furnace, and two steel soaking pits. The exposures involved numerous thermal cycles, temperatures in the range 925 to 1250°C, and exposure periods of 530 to 5545 h. The principal observations and/or conclusions derived from examination of the exposed specimens follow.

- Specimens exposed in the aluminum remelt furnaces were covered with glassy deposits and (in one case) with loosely adhering deposits. The principal constituents in these deposits were Al, K, Na, and Si.

- Surface recession rates measured in Hexoloy SA, NC-400, NC-430, and SC-X exposed to aluminum remelt furnace No. 1 were 0.1 to 0.6 mm/y (0.004 to 0.024 in./y). Corrosion appeared to be general in nature. The Si phase in siliconized and reaction sintered SiC was not selectively attacked. Although not measured, surface recession was also inferred by microstructural changes in Si_3N_4-bonded SiC ceramics exposed to aluminum

remelt furnaces. On the other hand, none of the SiC ceramics corroded significantly in the other three furnaces.

- Surface recession rates in steel soaking pit No. 2 were 3.5 mm/y (0.14 in./y) for Hexoloy SA and Sintride, 4.2 mm/y (0.17 in./y) for NC-430 and KT, and 6.8 mm/y (0.27 in./y) for C/75. Corrosion and/or erosion was higher in this furnace than in any other.

- Little or no surface recession occurred in the forge and steel reheat furnace and in steel soaking pit No. 1. In these furnaces the environment was evidently much less aggressive, possibly because of specimen location in soaking pit No. 1.

- The average C-ring fracture strength of Hexoloy SA was lowest for specimens exposed to an aluminum remelt furnace wherein significant surface recession occurred. The average C-ring fracture strength of NC-430, however, was lowest for specimens exposed in steel soaking pit No. 1 wherein minimum surface recession occurred. These data show that exposure to different furnace environments causes different degrees of strength degradation.

- Macroscopic cracking occurred in the Si_3N_4-bonded SiC specimens in most tests. These materials also exhibited larger weight gains than other SiC ceramics.

ACKNOWLEDGMENTS

The authors wish to acknowledge and thank those who assisted in the performance of the work and preparation of the report: A. C. Schaffhauser and E. L. Long for guidance and support; P. J. Jones for initial inspection of exposed specimens, cutting of samples, and measurement of fracture strengths; O. B. Cavin for x-ray diffraction studies; L. Landau for spectroscopic analyses; J. R. Mayotte for ceramographic preparation and photomicrographs: T. J. Henson for electron microprobe analyses; M. K. Ferber and E. L. Long for technical review and helpful suggestions; J. P. Hickey for preparation of figures; F. W. Burns for typing draft; and H. G. Sharpe for preparation of the final manuscript.

REFERENCES

1. J. J. Cleveland, J. M. Gonzalez, and K. H. Kohnken, *Ceramic Heat Recuperators for Industrial Heat Recovery*, DOE/EC/02162, August 1980.

2. G. C. Fay and K. H. Kohnken, "Development and Potential in the Ceramic Industry of the High Temperature Ceramic Recuperator Body," *Ceram. Bull.* 62(9), September 1983.

3. *An Assessment of Ceramic Materials Technology for Heat Exchangers*, EGG-SE-6367, January 1984.

4. J. W. Bjerklie and R. A. Penty, *High Temperature Recuperator Tests*, DOE Contract No. DE-ACOZ-79 S-40257, Hague International, May 1980.

5. A. O. Hoffman, H. W. Lownie, and F. C. Holden, *An Energy Audit of Three Energy-Conserving Devices in a Steel Industry Demonstration Program. Task III: GTE High Temperature Recuperator*, Final Report, Battelle Columbus Laboratories, Columbus, Ohio, January 1983.

6. H. W. Lownie and F. C. Holden, *An Energy Audit of Three Energy-Conserving Devices in a Steel-Industry Demonstration Program, Task I, Hague Forge Furnaces*, PNL-4636, February 1983.

7. M. Coombs, D. Kotchick, and H. Strumpf, *High-Temperature Burner-Duct-Recuperator (HTBDR) Program: Annual Report, October 1981 through September 1982*, DOE/ID/12170, May 1983.

8. *High-Temperature Burner-Duct-Recuperator System Evaluation, Annual Report: October 1981–September 1982*, LRC 5282, Babcock & Wilcox Company, January 1984.

9. M. K. Ferber and V. J. Tennery, "Behavior of Tubular Ceramic Heat Exchanger Materials in Basic Coal Ash from Coal-Oil-Mixture Combustion," *Bull. Am. Ceram. Soc.* 63(7), 898–904 (1984).

10. M. K. Ferber and V. J. Tennery, *Evaluation of Tubular Ceramic Heat Exchanger Materials in Acidic Coal Ash from Coal-Oil-Mixture Combustion*, ORNL/TM-7958, p. 28–29, December 1981.

11. A. D. Russell, C. E. Smeltzer, and M. E. Ward, *Waste Heat Recuperation for Aluminum Furnaces*, GRI-81/0160, April 1983.

12. R. E. Tressler, M. D. Meiser, and T. Yonushonis, "Molten Salt Corrosion of SiC and Si_3N_4 Ceramics," *J. Am. Ceram. Soc.* 59(5–6), 278 (May–June 1976).

13. J. A. Coppola, M. Srinivasan, K. T. Faber, and R. H. Smoak, *High Temperature Properties of Sintered Alpha Silicon Carbide*, The Carborundum Company, Niagara Falls, N.Y., 1979.

14. J. W. Lucek, M. L. Torti, G. Q. Weaver, and B. A. Olson, *Cast Densified Silicon Carbides*, paper No. 790253 presented at The Society of Automotive Engineers, Inc. Congress and Exposition, Feb. 26–Mar. 2, 1979.

ORNL/TM-9677
Dist. Category
UC-95

INTERNAL DISTRIBUTION

1–2. Central Research Library
3. Document Reference Section
4–5. Laboratory Records Department
6. Laboratory Records, ORNL RC
7. ORNL Patent Section
8. P. Angelini
9. R. A. Bradley
10. A. J. Caputo
11. R. S. Carlsmith
12. P. T. Carlson
13. F. C. Chen
14. J. H. DeVan
15–24. J. I. Federer
25. H. W. Hoffman
26. M. A. Janney
27. D. R. Johnson
28. R. R. Judkins
29. E. L. Long, Jr.
30. A. J. Moorhead
31. A. C. Schaffhauser
32. J. L. Scott
33. D. P. Stinton
34–36. P. T. Thornton
37–41. T. N. Tiegs
42. R. J. Charles (Consultant)
43. H. E. Cook (Consultant)
44. Alan Lawley (Consultant)
45. T. B. Massalski (Consultant)
46. R. L. Smith (Consultant)
47. J. C. Williams (Consultant
48. K. M. Zwilsky (Consultant)

EXTERNAL DISTRIBUTION

49–50. AEROJET ENERGY CONVERSION COMPANY, P.O. Box 13222, Sacramento, CA 95813

L. Hoffman
H. W. Williams

51–56. AIRESEARCH MANUFACTURING COMPANY, 2525 W. 190th Street, Torrance, CA 90509

M. G. Coombs
D. M. Kotchick (5)

57–62. BABCOCK AND WILCOX, P.O. Box 239, Lynchburg, VA 24505

D. Petrak (5)
J. E. Snyder

63. C&H COMBUSTION, 1104 E. Big Beaver Road, Troy, MI 48083

R. G. Graham

64. CABOT CORPORATION, 1020 West Park Avenue, Kokomo, IN 46901

M. F. Rothman

65. COMBUSTION ENGINEERING, INC., 911 West Main Street, Chattanooga, TN 37402

C. H. Sump

66. CONSOLIDATED NATURAL GAS, 11001 Cedar Avenue, Cleveland, OH 44106

J. Bjerklie

67–69. COORS PORCELAIN COMPANY, 600 Ninth Street, Golden, CO 80401

C. Dobos
R. Kleiner
D. Roy

70. GAS RESEARCH INSTITUTE, 8600 West Bryn Mawr Avenue, Chicago, IL 60631

W. W. Liang

71–72. GTE PRODUCTS CORPORATION, Hawes Street, Townada, PA 18848

J. L. Ferri
J. Gonzalez

73. HAGUE INTERNATIONAL, 3 Adams Street, South Portland, MA 04106

S. B. Young

74–75. IIT RESEARCH INSTITUTE, 10 West 35th Street, Chicago, IL 60616

J. W. Adams
D. C. Larsen

76–77. NORTON COMPANY, Worcester, MA 01606

B. D. Foster
M. L. Torti

78. PENNSYLVANIA STATE UNIVERSITY, 201 Steidle Building, University Park, PA 16802

R. E. Tressler

79–81. SOLAR TURBINES INCORPORATED, P.O. Box 85376, San Diego, CA 92138-5376

T. A. Argabright
C. E. Smeltzer
M. E. Ward

82. SOHIO ENGINEERED MATERIALS COMPANY, Structural Ceramics Division, P.O. Box 10549, Niagara Falls, NY 14302

J. Halstead

83–84. THERMO ELECTRON COMPORATION, P.O. Box 459, Waltham, MA 02254

W. E. Cole
R. DeSaro

85. UNIVERSITY OF ILLINOIS AT CHAMPAIGN-URBANA, 105 W. Goodwin Avenue, Urbana, IL 61801

M. K. Ferber

86. UNIVERSITY OF ILLINOIS AT CHICAGO, P.O. Box 4348, Chicago, IL 60680

M. J. McNallan

87–89. DOE, IDAHO OPERATIONS OFFICE, 550 2nd Street, Idaho Falls, ID 83401

F. Childs
J. B. Patton
W. H. Thielbar

90–93. DOE, OFFICE OF INDUSTRIAL CONSERVATION, 1000 Independence Avenue, Forrestal Building, Washington, DC 20585

A. J. Hayes
S. L. Richlen
J. R. Rossmeissl
W. B. Williams, Director

94. Office of Asst. Manager for Energy R&D, DOE-ORO

95-216. DOE, TECHNICAL INFORMATION CENTER, Office of Information Services, P.O. Box 62, Oak Ridge, TN 37831

For distribution as shown in DOE/TIC-4500, Distribution Category UC-95 (Energy Conservation).

*U. S. GOVERNMENT PRINTING OFFICE: 1985-544-045/20108